Molecular Cell

Article

A GAPDH serotonylation system couples CD8$^+$ T cell glycolytic metabolism to antitumor immunity

Graphical abstract

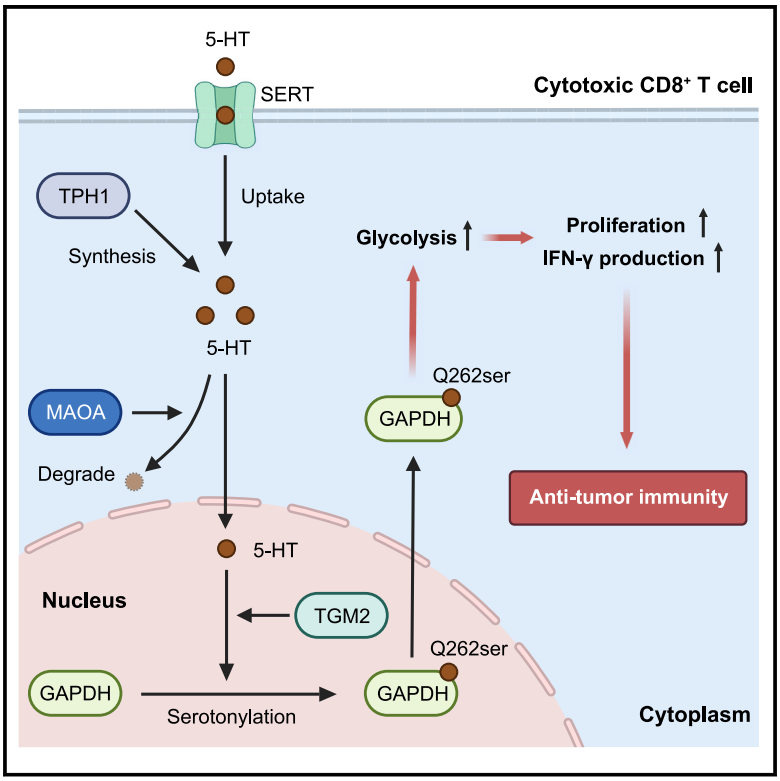

Highlights

- TGM2-induced serotonylation of GAPDH Q262 promotes CD8$^+$ T cell glycolytic metabolism
- GAPDH Q262 serotonylation enhances CD8$^+$ T cell antitumor immune activity
- CD8$^+$ T cells accumulate 5-HT for serotonylation via TPH1 generation and SERT uptake
- 5-HT-producing TPH1-CAR-T cells have potent antitumor activity

Authors

Xu Wang, Sheng-Qiao Fu, Xiao Yuan, ..., Li-Peng Hu, Xue-Li Zhang, Zhi-Gang Zhang

Correspondence

jsdxwx@126.com (X.W.), xuzhang@ujs.edu.cn (X.Z.), shjiang@shsci.org (S.-H.J.), lphu@shsci.org (L.-P.H.), xlzhang@shsci.org (X.-L.Z.), zzhang@shsci.org (Z.-G.Z.)

In brief

As a neurotransmitter, serotonin (5-HT) has multiple roles in regulating immune responses. Although canonical 5-HT-receptor signaling has been well characterized, Wang et al. show that the post-translational serotonylation of GAPDH Q262 promotes CD8$^+$ T cell glycolytic metabolism and antitumor immune activity. 5-HT-producing CAR-T cells have potent antitumor activity.

Wang et al., 2024, Molecular Cell *84*, 1–16
February 15, 2024
https://doi.org/10.1016/j.molcel.2023.12.015

CellPress

Please cite this article in press as: Wang et al., A GAPDH serotonylation system couples CD8+ T cell glycolytic metabolism to antitumor immunity, Molecular Cell (2023), https://doi.org/10.1016/j.molcel.2023.12.015

Molecular Cell

CellPress

Article

A GAPDH serotonylation system couples CD8+ T cell glycolytic metabolism to antitumor immunity

Xu Wang,[1,5,*] Sheng-Qiao Fu,[1,5] Xiao Yuan,[1,5] Feng Yu,[3,5] Qian Ji,[1,5] Hao-Wen Tang,[1,5] Rong-Kun Li,[1] Shan Huang,[2] Pei-Qi Huang,[2] Wei-Ting Qin,[2] Hao Zuo,[3] Chang Du,[2] Lin-Li Yao,[2] Hui Li,[2] Jun Li,[2] Dong-Xue Li,[2] Yan Yang,[2] Shu-Yu Xiao,[2] Aziguli Tulamaiti,[2] Xue-Feng Wang,[1] Chun-Hua Dai,[1] Xu Zhang,[4,*] Shu-Heng Jiang,[2,*] Li-Peng Hu,[2,*] Xue-Li Zhang,[2,*] and Zhi-Gang Zhang[2,6,*]

[1]Department of Radiation Oncology, Cancer Institute of Jiangsu University, Affiliated Hospital of Jiangsu University, Zhenjiang 212001, P.R. China

[2]State Key Laboratory of Systems Medicine for Cancer, Shanghai Cancer Institute, Ren Ji Hospital, School of Medicine, Shanghai Jiao Tong University, Shanghai 200240, P.R. China

[3]School of Life Sciences, Jiangsu University, Zhenjiang 212013, P.R. China

[4]Jiangsu Key Laboratory of Medical Science and Laboratory Medicine, School of Medicine, Jiangsu University, Zhenjiang 212013, P.R. China

[5]These authors contributed equally

[6]Lead contact

*Correspondence: jsdxwx@126.com (X.W.), xuzhang@ujs.edu.cn (X.Z.), shjiang@shsci.org (S.-H.J.), lphu@shsci.org (L.-P.H.), xlzhang@shsci.org (X.-L.Z.), zzhang@shsci.org (Z.-G.Z.)

https://doi.org/10.1016/j.molcel.2023.12.015

SUMMARY

Apart from the canonical serotonin (5-hydroxytryptamine [5-HT])-receptor signaling transduction pattern, 5-HT-involved post-translational serotonylation has recently been noted. Here, we report a glyceraldehyde-3-phosphate dehydrogenase (GAPDH) serotonylation system that promotes the glycolytic metabolism and antitumor immune activity of CD8+ T cells. Tissue transglutaminase 2 (TGM2) transfers 5-HT to GAPDH glutamine 262 and catalyzes the serotonylation reaction. Serotonylation supports the cytoplasmic localization of GAPDH, which induces a glycolytic metabolic shift in CD8+ T cells and contributes to antitumor immunity. CD8+ T cells accumulate intracellular 5-HT for serotonylation through both synthesis by tryptophan hydroxylase 1 (TPH1) and uptake from the extracellular compartment via serotonin transporter (SERT). Monoamine oxidase A (MAOA) degrades 5-HT and acts as an intrinsic negative regulator of CD8+ T cells. The adoptive transfer of 5-HT-producing TPH1-overexpressing chimeric antigen receptor T (CAR-T) cells induced a robust antitumor response. Our findings expand the known range of neuroimmune interaction patterns by providing evidence of receptor-independent serotonylation post-translational modification.

INTRODUCTION

Serotonin (5-hydroxytryptamine [5-HT]) is a monoamine neurotransmitter that regulates both neural and other biological functions in the central nervous system and peripheral tissues.[1] Tryptophan hydroxylases (TPHs), including TPH1 and TPH2, are the rate-limiting enzymes for 5-HT synthesis in mammals.[2] The expression of TPH1 is abundant in peripheral tissues, whereas the expression of TPH2 is restricted to the nervous system.[2] Outside the blood-brain barrier, peripheral 5-HT generated by TPH1 has been reported to provide an essential link between serotonergic signals and tumor progression. Previous studies from our group and others have shown the stimulatory effect of 5-HT on tumor progression by directly promoting tumor cell growth and invasion.[3,4] Interestingly, recent studies have indicated that 5-HT can also exert biological effects by acting on immune cells that infiltrate in the tumor microenvironment.[5,6] However, the detailed molecular mechanism by which 5-HT mediates CD8+ T cell antitumor immunity remains elusive.

5-HT exerts its function by binding to plasma membrane 5-HT receptors (5-HTRs) or being covalently incorporated into proteins via transamidation; the latter is a newly recognized post-translational modification known as serotonylation.[7] Transglutaminases (TGMs) are necessary to catalyze the serotonylation reaction by transferring 5-HT to the glutamine (Gln) residues of target proteins.[8] Since the initial discovery of serotonylation in platelets, accumulating evidence has highlighted its occurrence in various cell types, including nerve cells, smooth muscle cells, pancreatic β-cells, and even in the extracellular matrix.[8,9] CD8+ T cells have been shown to express components of the serotonergic system, including the 5-HT synthetase TPH1, the 5-HT catabolic enzyme monoamine oxidase A (MAOA), and the serotonylation enzyme TGM2.[6,10] However, whether serotonylation participates in CD8+ T cell activation and antitumor immunity remains unclear.

Please cite this article in press as: Wang et al., A GAPDH serotonylation system couples CD8+ T cell glycolytic metabolism to antitumor immunity, Molecular Cell (2023), https://doi.org/10.1016/j.molcel.2023.12.015

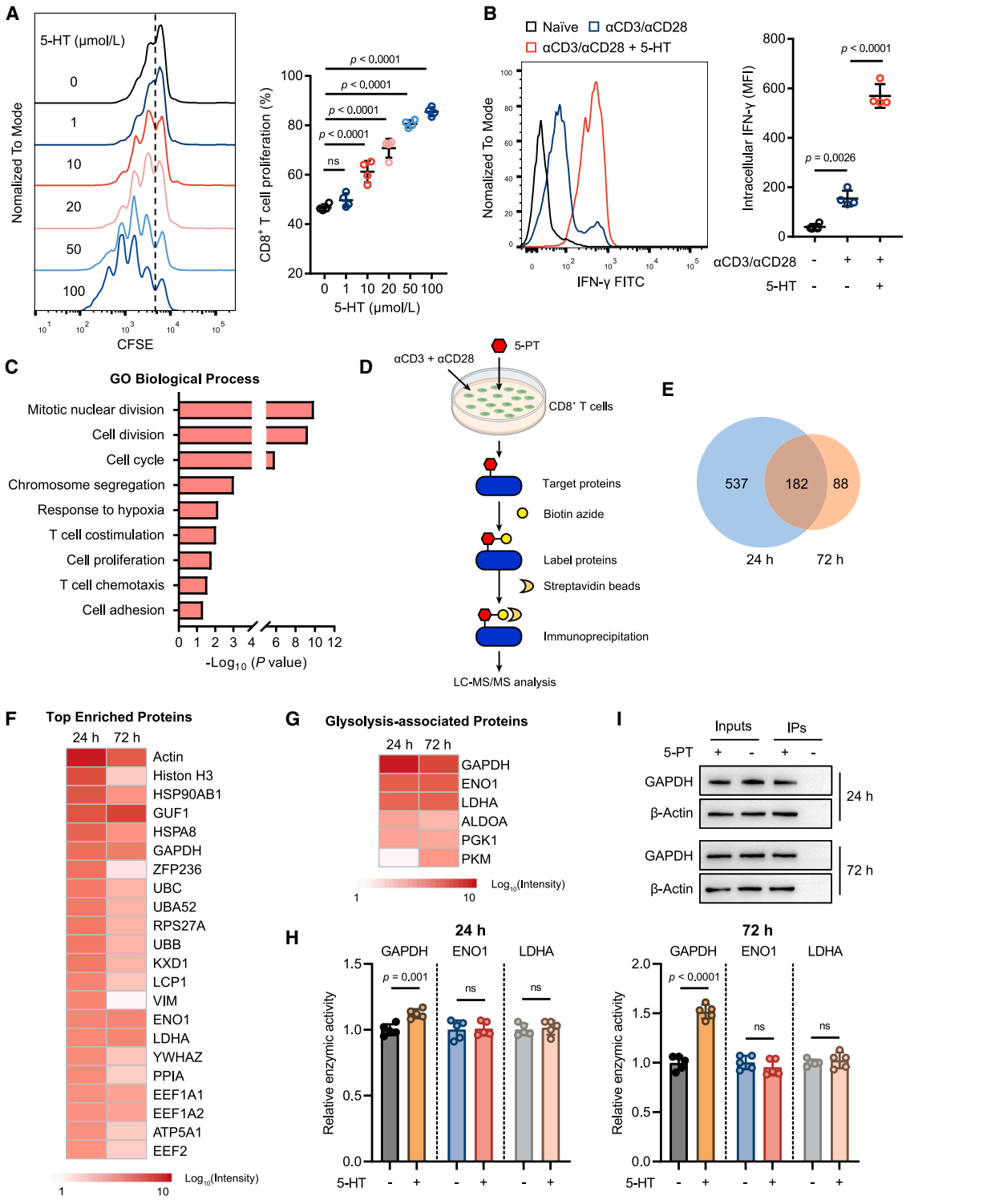

Figure 1. 5-HT promotes CD8+ T cell activation and induces GAPDH serotonylation

(A and B) CD8+ T cells were activated for 72 h, with 1, 10, 20, 50, or 100 μmol/L 5-HT. Cell proliferation (A) and intracellular IFN-γ (B) (100 μmol/L 5-HT) were determined (n = 4 per group, 3 independent experiments).

(C) CD8+ T cells were activated for 24 h, with or without 100 μmol/L 5-HT. RNA sequencing was performed, followed by Gene Ontology (GO) biological process analysis (n = 3 per group, 1 independent experiment).

(D) Workflow for the discovery of serotonylated proteins by LC-MS/MS.

(legend continued on next page)

In this study, we determined that 5-HT-induced serotonylation of glyceraldehyde-3-phosphate dehydrogenase (GAPDH) could promote CD8$^+$ T cell activation. TGM2 was proven to be essential for the serotonylation reaction. Gln262, residing in the nuclear export signal (NES) of GAPDH, was identified as the serotonylation site, which facilitated GAPDH cytoplasmic localization and glycolytic activity. Metabolic adaptation to glycolysis supported CD8$^+$ T cell activation and antitumor immune responses. Activated CD8$^+$ T cells accumulated intracellular 5-HT for serotonylation through endogenous generation by TPH1 and uptake from the extracellular compartment via serotonin transporter (SERT). MAOA acted as a negative regulator of CD8$^+$ T cells by degrading intracellular 5-HT and suppressing GAPDH serotonylation. These results reveal an intrinsic serotonylation post-translational modification system that enhances the antitumor immune activity of CD8$^+$ T cells.

RESULTS

5-HT promotes CD8$^+$ T cell activation and induces GAPDH serotonylation

Recent evidence has revealed that 5-HT provides essential links in the transduction of neuroimmune signaling.[11] To further explore the involvement of peripheral 5-HT in antitumor immune responses, we first assessed whether peripheral 5-HT could affect immune cell development. The absolute cell number and populations of CD8$^+$ and CD4$^+$ T lymphocytes, myeloid Ly6C$^+$CD11b$^+$ monocytes/macrophages, and Ly6G$^+$CD11b$^+$ neutrophils were examined in the thymus, bone marrow, spleen, lymph nodes, and blood of wild-type (WT) and peripheral 5-HT-deficient *Tph1*$^{-/-}$ mice. We found that the absolute number (Figure S1A) and frequency of immune cell populations (Figure S1B) were similar between WT and *Tph1*$^{-/-}$ mice. Naïve, memory, and effector subsets of CD8$^+$ and CD4$^+$ T lymphocytes in the spleen also displayed no significant differences between the two groups (Figure S1C). This suggests that peripheral 5-HT may not be involved in the development of immune cell populations under physiological conditions.

Next, the direct effect of 5-HT on CD8$^+$ T cell activation was assessed *in vitro*. We observed that 5-HT could directly promote the αCD3/αCD28-stimulated cellular proliferation of CD8$^+$ T cells (Figure 1A). In addition, intracellular staining revealed that interferon (IFN)-γ production was elevated by 5-HT (Figure 1B). Unbiased high-throughput RNA sequencing (RNA-seq) was then performed to compare the transcriptional variations induced by 5-HT. Principal-component analysis (PCA) revealed the major differences among naïve, non-5-HT-treated, and 5-HT-treated CD8$^+$ T cells (Figure S1D). Functional enrichment analysis further confirmed that 5-HT intensively promoted the expression of CD8$^+$ T cell activation-associated genes (Figure 1C).

Serotonylation refers to the covalent transamidation of 5-HT to protein Gln residues.[8] CD8$^+$ T cells have been shown to express TGMs; however, whether they can catalyze the serotonylation reaction is unknown. Propargylated 5-HT (5-PT) is an alkyne-functionalized 5-HT derivative that can be taken up into living cells and acts as a substrate for serotonylation.[8] We observed that 5-PT was able to promote CD8$^+$ T cell activation, verifying its biological activity (Figure S1E). Using copper-click chemistry, biotin-bonded 5-PT was immunoprecipitated to identify protein serotonylation in CD8$^+$ T cells with targeted liquid chromatography-tandem mass spectrometry (LC-MS/MS) (Figure 1D). At 24 and 72 h, 719 and 270 proteins were identified, respectively, with 182 proteins detected at both 24 h (25.3%) and 72 h (66.6%) (Figure 1E and Table S1). A heatmap of the top enriched proteins in the overlapping set revealed the proteins previously confirmed to be serotonylated, including Actin and Histone H3 (Figure 1F).[9] Metabolic reprogramming toward aerobic glycolysis is concomitant with the activation of CD8$^+$ effector T cells.[12] Interestingly, we identified several glycolysis-associated proteins in 5-PT-immunoprecipitated substrates (Figure 1G). GAPDH, enolase 1 (ENO1), and lactate dehydrogenase A (LDHA) were the top three enriched enzymes, displaying a more than 3-fold increase compared with other enzymes (Figure 1G). By measuring the enzymatic activity of the top three enriched glycolysis-associated enzymes, we observed that GAPDH activity but not ENO1 nor LDHA activity was enhanced by 5-HT (Figure 1H), suggesting a potential role of 5-HT in promoting GAPDH activity. Western blotting analyses were performed to confirm the results of serotonylation revealed by LC-MS/MS. β-actin was previously identified as the serotonylation substrate.[13,14] We found that 5-PT-induced β-actin serotonylation signal was detected (Figure 1I). Moreover, the serotonylation signal of GAPDH was also detected (Figure 1I). This finding indicates that GAPDH is the substrate for serotonylation, and GAPDH serotonylation may be associated with enhanced glycolytic metabolism in activated CD8$^+$ T cells.

Serotonylation of GAPDH promotes the glycolytic metabolism and antitumor activity of CD8$^+$ T cells

TGMs catalyze the serotonylation reaction by transferring 5-HT to the Gln residues of target proteins.[15] TGM family members include TGM1–TGM7. Unbiased RNA-seq and real-time qPCR showed that TGM2 was the most highly expressed TGM in both naïve and activated CD8$^+$ T cells (Figures 2A and 2B). To assess whether TGM2-involved serotonylation is essential for 5-HT-induced CD8$^+$ T cell activation, the TGM2 inhibitor LDN-27219 was used. We observed that 5-HT-induced CD8$^+$

(E) Venn diagram showing the overlap of serotonylated proteins between 24 and 72 h in activated CD8$^+$ T cells.
(F and G) Heatmap of the top enriched proteins (F) and glycolysis-associated proteins (G) among the 182 commonly enriched proteins.
(H) CD8$^+$ T cells were activated for 24 and 72 h, with or without 100 μmol/L 5-HT. Activities of GAPDH, ENO1, and LDHA were assessed (n = 5 per group, 3 independent experiments).
(I) CD8$^+$ T cells were activated for 24 and 72 h, with or without 100 μmol/L 5-PT. 5-PT was immunoprecipitated, and GAPDH were detected (n = 1 per group, 3 independent experiments). IP, immunoprecipitation.
Bars represent mean ± standard deviation. ns indicates not significant.
See also Figure S1 and Table S1.

Please cite this article in press as: Wang et al., A GAPDH serotonylation system couples CD8+ T cell glycolytic metabolism to antitumor immunity, Molecular Cell (2023), https://doi.org/10.1016/j.molcel.2023.12.015

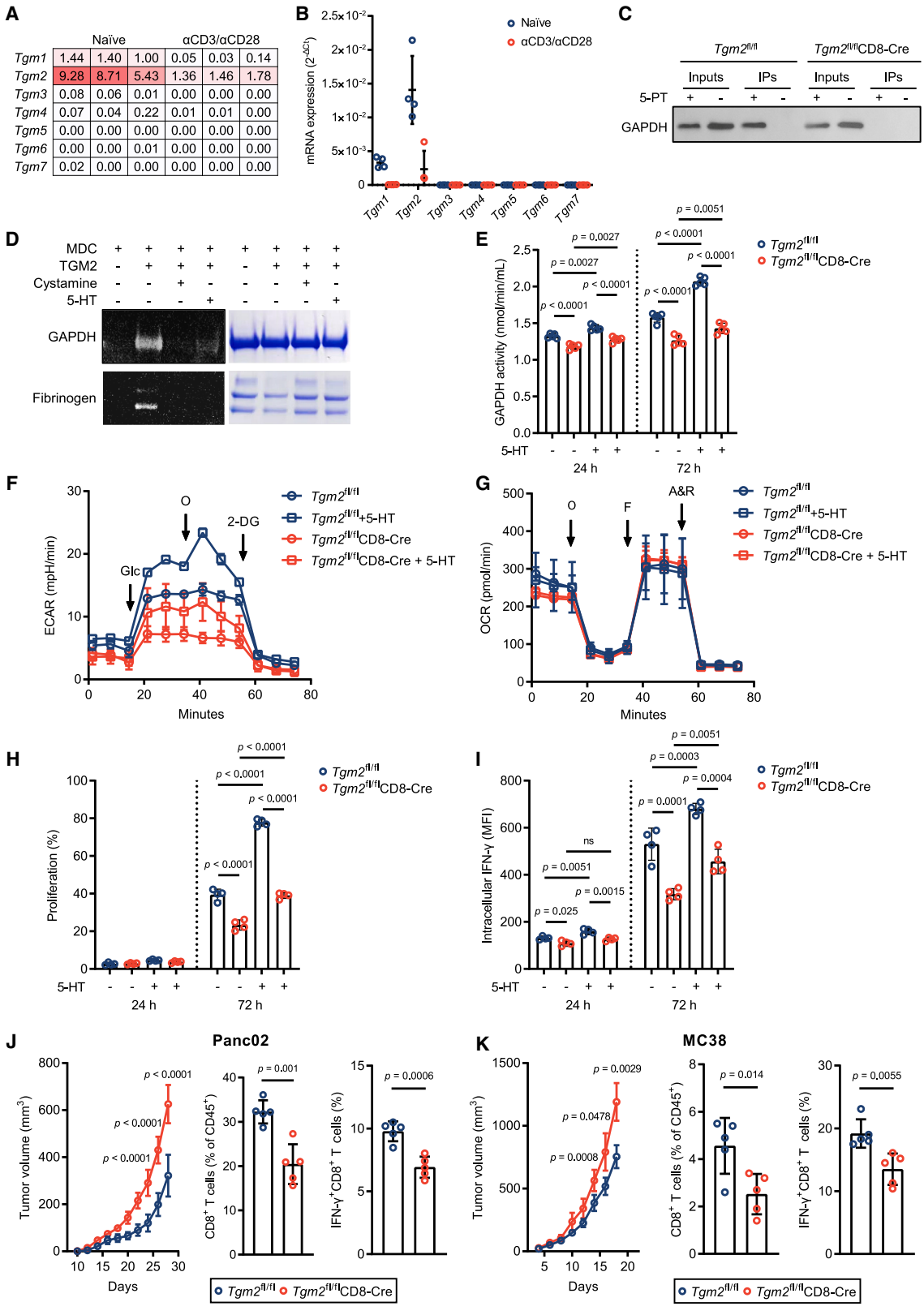

	Naïve			αCD3/αCD28		
Tgm1	1.44	1.40	1.00	0.05	0.03	0.14
Tgm2	9.28	8.71	5.43	1.36	1.46	1.78
Tgm3	0.08	0.06	0.01	0.00	0.00	0.00
Tgm4	0.07	0.04	0.22	0.01	0.01	0.00
Tgm5	0.00	0.00	0.00	0.00	0.00	0.00
Tgm6	0.00	0.00	0.01	0.00	0.00	0.00
Tgm7	0.02	0.00	0.00	0.00	0.00	0.00

(legend on next page)

Please cite this article in press as: Wang et al., A GAPDH serotonylation system couples CD8+ T cell glycolytic metabolism to antitumor immunity, Molecular Cell (2023), https://doi.org/10.1016/j.molcel.2023.12.015

T cell activation was inhibited by the TGM2 inhibitor (Figure S2A). Functional enrichment analysis of the RNA-seq data further revealed that immune response-associated functions were impaired by the TGM2 inhibitor (Figure S2B). To confirm the role of TGM2, we generated CD8+ T cell conditional TGM2-knockout (*Tgm2*$^{flox/flox}$*Cd8a*^{cre}, *Tgm2*$^{fl/fl}$CD8-Cre) mice (Figure S2C). Compared with *Tgm2*$^{fl/fl}$ CD8+ T cells, no serotonylation signal was detected in TGM2-deficient *Tgm2*$^{fl/fl}$CD8-Cre CD8+ T cells (Figure 2C). Monodansylcadaverine (MDC), a fluorescent monoamine analog, was used for *in vitro* detection of the serotonylation of GAPDH in the presence of the TGM2 protein. The results confirmed that TGM2-induced transamidation of MDC signals was obtained on GAPDH and fibrinogen (Figure 2D), a protein previously demonstrated to be serotonylated.[16] The TGM inhibitor or competition with 5-HT attenuated the transamidation of MDC (Figure 2D).

Considering the recently noted role of glycolytic metabolism in CD8+ T cell activation,[12] serotonylation of GAPDH in this process was investigated. By measuring GAPDH catalytic activity at 24 and 72 h after CD8+ T cell activation, we observed that GAPDH activity was reduced in TGM2-deficient *Tgm2*$^{fl/fl}$CD8-Cre cells compared with *Tgm2*$^{fl/fl}$ cells (Figure 2E). 5-HT was able to increase GAPDH activity in *Tgm2*$^{fl/fl}$ CD8+ T cells, whereas this effect was weakened in TGM2-depleted cells (Figure 2E). In addition, extracellular acidification (ECAR) metabolic analyses confirmed the enhanced glycolytic metabolism in 5-HT-stimulated CD8+ T cells, but knockout of TGM2 inhibited it (Figures 2F and S2D). Oxidative phosphorylation, indicated by oxygen consumption rate (OCR), was not altered by 5-HT, and no significant differences were observed between *Tgm2*$^{fl/fl}$ and *Tgm2*$^{fl/fl}$CD8-Cre CD8+ T cells (Figures 2G and S2E). The GAPDH inhibitor heptelidic acid (HA) and glycolytic inhibitor 2-deoxy-D-glucose (2-DG) blocked the proliferation and IFN-γ production of CD8+ T cells (Figures S2F and S2G), which indicated that GAPDH-involved glycolytic metabolism was essential for the activation of CD8+ T cells.

Next, TGM2-induced GAPDH serotonylation in CD8+ T cell activation was assessed. Compared with *Tgm2*$^{fl/fl}$ CD8+ T cells, we observed that cell proliferation and intracellular IFN-γ in TGM2-depleted *Tgm2*$^{fl/fl}$CD8-Cre cells were suppressed (Figures 2H and 2I). In addition, 5-HT-enhanced cell activation was reduced in *Tgm2*$^{fl/fl}$CD8-Cre CD8+ T cells (Figures 2H and 2I). To validate the *in vivo* effects of TGM2 on antitumor immunity, Panc02 and MC38 tumor cells were subcutaneously implanted into *Tgm2*$^{fl/fl}$ and *Tgm2*$^{fl/fl}$CD8-Cre mice. Knockout of TGM2 had no effect on the accumulation of intracellular 5-HT in CD8+ T cells or tumor cells, indicating that 5-HT availability was not altered (Figures S2H and S2I). Measuring the tumor volume, we observed that Panc02 and MC38 tumors grew more vigorously in TGM2-deficient *Tgm2*$^{fl/fl}$CD8-Cre mice (Figures 2J and 2K). Infiltration of intratumoral CD8+ T cells was reduced in *Tgm2*$^{fl/fl}$CD8-Cre mice (Figures 2J, 2K, S2J, and S2K). By detecting intracellular IFN-γ in tumor-infiltrating CD8+ T cells, we found that TGM2-deficient CD8+ T cells expressed less IFN-γ than *Tgm2*$^{fl/fl}$ CD8+ T cells (Figures 2J, 2K, S2L, and S2M). To exclude the possibility that CD4+ T cells could induce indirect antitumor effects *in vivo*, we depleted CD4+ T cells in *Tgm2*$^{fl/fl}$ and *Tgm2*$^{fl/fl}$CD8-Cre mice using an anti-CD4 antibody. Compared with that in *Tgm2*$^{fl/fl}$ mice, tumor growth was still accelerated in CD4+ T cell-depleted *Tgm2*$^{fl/fl}$CD8-Cre mice (Figures S2N and S2O). These results suggest that TGM2-mediated serotonylation contributes to CD8+ T cell activation and antitumor immunity.

Serotonylation of Gln262 at GAPDH NES facilitates its cytoplasmic location and glycolytic activity in CD8+ T cells

To identify the site(s) of serotonylation on GAPDH, LC-MS/MS following *in vitro* TGM2 assays with MDC was performed. Peptide tandem mass spectrometry revealed that Gln residues at positions 46, 76, 183, 202, and 262 but not 278 could be serotonylated in synthesized mouse GAPDH peptides (Figures 3A and S3A–S3E). Further analysis using the full-length GAPDH protein revealed Gln183 and 262 as the reactive substrates for serotonylation (Figures 3B and S3F). We noticed that Gln(Q)262 resides in the NES sequence ^{257}KKVVKQASEGPLK^{269} of GAPDH.[17] Glycolytic activity of GAPDH is related to its subcellular localization, and translocation of GAPDH from the nucleus to the cytoplasm determines its efficient enzymatic activity.[18] GAPDH lacks a nuclear localization signal (NLS)[19]; therefore, modification of the NES is essential for GAPDH localization. NES of GAPDH is highly conserved across different species (Figure 3C). Peptide

Figure 2. Serotonylation of GAPDH promotes the glycolytic metabolism and antitumor activity of CD8+ T cells

(A and B) CD8+ T cells were activated for 24 h. *Tgms* mRNA expression was analyzed by RNA sequencing (A, n = 3 per group, 1 independent experiment) and real-time qPCR (B, n = 4 per group, 3 independent experiments).

(C) *Tgm2*$^{fl/fl}$ or *Tgm2*$^{fl/fl}$CD8-Cre CD8+ T cells were activated for 24 h, with or without 100 μmol/L 5-PT. 5-PT was immunoprecipitated, and GAPDH were detected (n = 1 per group, 3 independent experiments). IP, immunoprecipitation.

(D) TGM2 monoaminylation assays with GAPDH or fibrinogen in the presence or absence of 4 mmol/L TGM inhibitor (cystamine) or donor competition with excess 500 μmol/L 5-HT (n = 1 per group, 3 independent experiments).

(E) *Tgm2*$^{fl/fl}$ or *Tgm2*$^{fl/fl}$CD8-Cre CD8+ T cells were activated for 24 and 72 h, with or without 100 μmol/L 5-HT. GAPDH activity was detected (n = 5 per group, 2 independent experiments).

(F and G) *Tgm2*$^{fl/fl}$ or *Tgm2*$^{fl/fl}$CD8-Cre CD8+ T cells were activated for 24 h, with or without 100 μmol/L 5-HT. ECAR (F) and OCR (G) were measured (n = 4 per group, 3 independent experiments).

(H and I) *Tgm2*$^{fl/fl}$ or *Tgm2*$^{fl/fl}$CD8-Cre CD8+ T cells were activated for 24 and 72 h, with or without 100 μmol/L 5-HT. Cell proliferation (H) and intracellular IFN-γ (I) were detected (n = 4 per group, 3 independent experiments).

(J and K) Panc02 (J) or MC38 (K) cells were subcutaneously implanted into syngeneic *Tgm2*$^{fl/fl}$ or *Tgm2*$^{fl/fl}$CD8-Cre mice. Tumor volume was monitored every 2 days (n = 7 per group, 3 independent experiments). Frequency and intracellular IFN-γ of CD8+ T cells were detected (n = 5 per group, 3 independent experiments).

Bars represent mean ± standard deviation. ns indicates not significant.

See also Figure S2.

Please cite this article in press as: Wang et al., A GAPDH serotonylation system couples CD8+ T cell glycolytic metabolism to antitumor immunity, Molecular Cell (2023), https://doi.org/10.1016/j.molcel.2023.12.015

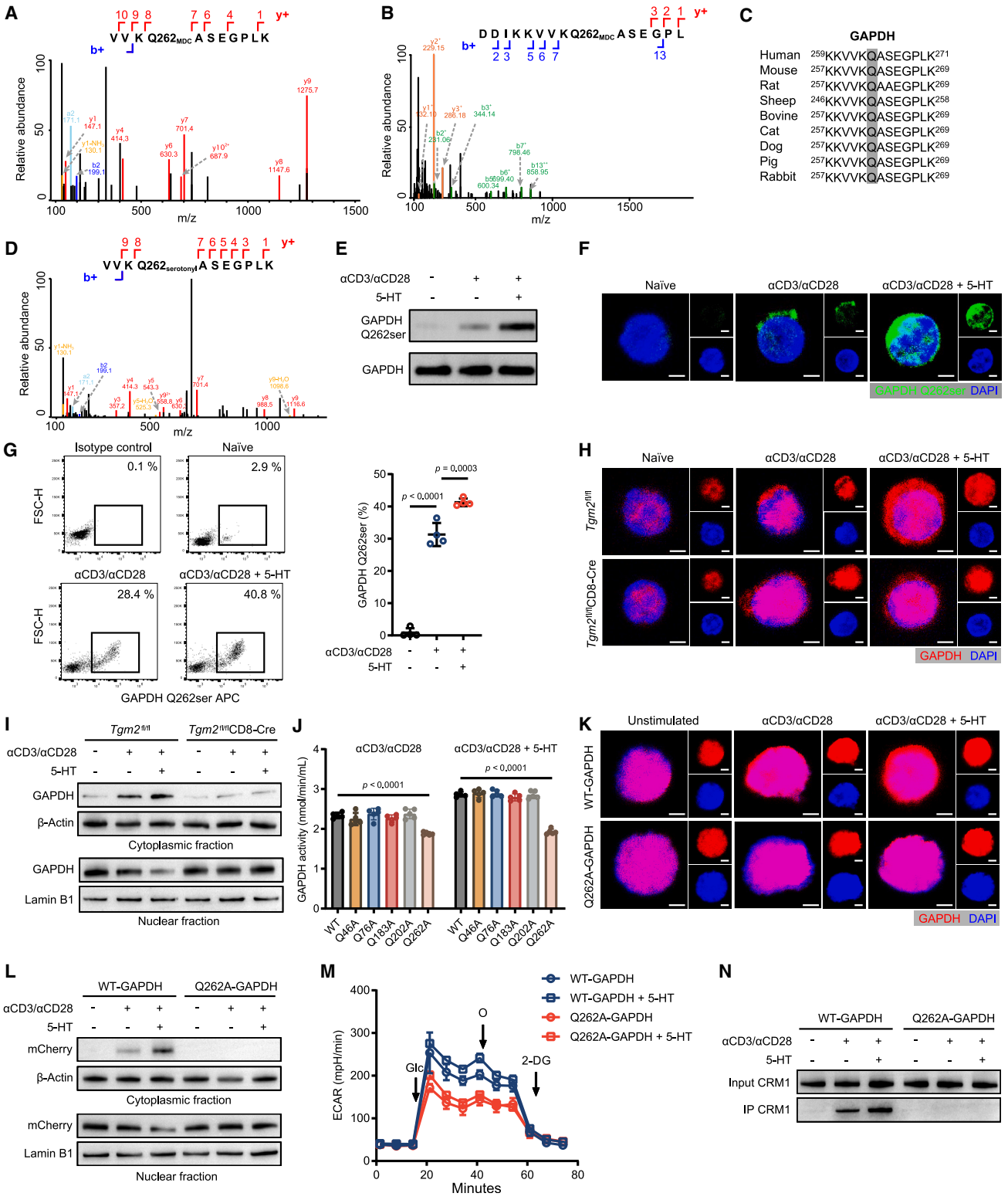

Figure 3. Serotonylation of Gln262 at GAPDH NES facilitates its cytoplasmic location and glycolytic activity in CD8+ T cells

(A and B) LC-MS/MS analysis of TGM2-transamidated MDC to GAPDH peptide 257–269 (A) and full-length GAPDH protein (B) (n = 1 per group, 3 independent experiments).

(C) The conserved GAPDH nuclear export signal sequence across different species.

(legend continued on next page)

Please cite this article in press as: Wang et al., A GAPDH serotonylation system couples CD8$^+$ T cell glycolytic metabolism to antitumor immunity, Molecular Cell (2023), https://doi.org/10.1016/j.molcel.2023.12.015

tandem mass spectrometry following an *in vitro* TGM2 assay with 5-HT further confirmed that GAPDH Gln262ser (Q262ser) was the direct substrate for TGM2-induced serotonylation (Figure 3D). To better characterize GAPDH serotonylation in CD8$^+$ T cells, we generated a GAPDH Q262ser modification-specific antibody. Peptide dot blot titration and immunoblotting analyses verified the reactivity of the GAPDH Q262ser antibody on Q262ser-modified peptide (Figure S3G) and full-length protein (Figure S3H). Western blotting experiments showed that weak GAPDH Q262ser modification was observed in naïve CD8$^+$ T cells (Figures 3E and S3I). αCD3/αCD28 stimulation promoted the serotonylation post-translational modification of GAPDH, which was further enhanced by the administration of 5-HT (Figures 3E and S3I). Confocal microscopy imaging also showed that serotonylated GAPDH Q262ser was barely expressed in naïve CD8$^+$ T cells (Figures 3F and S3J). αCD3/αCD28 stimulation induced the expression of GAPDH Q262ser in the cytoplasm rather than in the nucleus, and 5-HT further increased the expression of GAPDH Q262ser (Figures 3F and S3J). To quantify the percentage of GAPDH Q262ser serotonylation in CD8$^+$ T cells, flow cytometry analyses were performed by intracellularly staining GAPDH Q262ser. Results showed that less than 3% GAPDH Q262ser was detected in naïve CD8$^+$ T cells (Figure 3G). Activation with αCD3/αCD28 increased the percentage of GAPDH Q262ser to about 28.4%. 5-HT further increased the percentage of GAPDH Q262ser to about 40.8% (Figure 3G). Together, these data reveal the serotonylation of GAPDH Q262ser in activated CD8$^+$ T cells.

In light of the data supporting the serotonylation of GAPDH at NES, localization of GAPDH was visualized in CD8$^+$ T cells with a confocal microscope. We observed that GAPDH was mostly distributed in the nucleus of naïve CD8$^+$ T cells (Figures 3H and S3K). In activated CD8$^+$ T cells, cytoplastic distribution of GAPDH was observed, and 5-HT further promoted the translocation of GAPDH to the cytoplasm (Figures 3H and S3K). Nevertheless, in TGM2-deficient CD8$^+$ T cells, mobilization of GAPDH from the nucleus to the cytoplasm was impaired, even in the presence of 5-HT stimulation (Figures 3H and S3K). Consistent results were obtained from the immunoblotting analyses (Figures 3I and S3L). TGM2 was mainly expressed in the cytoplasm of naïve CD8$^+$ T cells, whereas nuclear expression of TGM2 was observed in activated CD8$^+$ T cells, suggesting the involvement of TGM2 in serotonylating nuclear proteins (Figures S3M and S3N).

To further validate the putative role of serotonylation in manipulating GAPDH activity, we generated mCherry-fused lentiviruses expressing either WT-GAPDH or Gln to Ala (Q46A, Q76A, Q183A, Q202A, and Q262A) mutated GAPDH and transduced them into murine T cell lymphoma EL4 cells. αCD3/αCD28 was used to stimulate EL4 cells, and enzymatic activity was analyzed. Results showed that GAPDH activity was only inhibited in Q262A-GAPDH mutated EL4 cells but not other mutated cells (Figure 3J). 5-HT-enhanced GAPDH activity was also suppressed in Q262A mutated GAPDH but not other mutations (Figure 3J). Confocal imaging (Figures 3K and S3O) and immunoblotting (Figures 3L and S3P) studies revealed that αCD3/αCD28 stimulation exported WT-GAPDH to the cytoplasm, and 5-HT further facilitated its transport. No apparent cytoplasmic translocation of Q262A-GAPDH was observed when cells were stimulated with αCD3/αCD28, which was minimally affected by 5-HT (Figures 3K, 3L, S3O, and S3P). In addition, in Q262A-GAPDH-expressing cells, 5-HT-ehnahced ECAR was significantly reduced (Figures 3M and S3Q), affirming the role of GAPDH Q262ser in CD8$^+$ T cell glycolytic metabolism.

Chromosome region maintenance 1 (CRM1, also called exportin 1) was reported to export the GAPDH protein by interacting with NES sequence.[17] In WT-GAPDH-transfected EL4 cells, immunoprecipitation analyses showed minimal interaction between WT-GAPDH and CRM1. αCD3/αCD28 activation promoted the binding of WT-GAPDH to CRM1, and 5-HT further enhanced their interaction (Figures 3N and S3R). However, in Q262A mutated GAPDH-transfected EL4 cells, interaction between CRM1 and GAPDH was weak, and αCD3/αCD28 activation had little effect on their interaction, even in the presence of 5-HT (Figures 3N and S3R). Several studies have demonstrated that cytoplasmic GAPDH possesses higher glycolytic activity than nuclear GAPDH.[20,21] Therefore, these findings indicate that serotonylation of GAPDH at Q262ser promotes the binding of GAPDH to exportin CRM1, which subsequently facilitates its cytoplasmic localization and glycolytic activity.

(D) LC-MS/MS analysis of TGM2-transamidated 5-HT to GAPDH peptide 257–269 (n = 1 per group, 3 independent experiments).
(E–G) CD8$^+$ T cells were activated for 24 h, with or without 100 μmol/L 5-HT. Serotonylation of GAPDH Q262ser was analyzed by western blotting (E, n = 1 per group, 3 independent experiments), confocal microscope (F, n = 10 for naïve group and n = 16 for other groups, 3 independent experiments), and flow cytometry (G, n = 4 per group, 3 independent experiments). Scale bars, 2 μm. An isotype antibody control was set for gating GAPDH Q262ser$^+$ cells.
(H and I) *Tgm2*$^{fl/fl}$ or *Tgm2*$^{fl/fl}$CD8-Cre CD8$^+$ T cells were activated for 24 h, with or without 100 μmol/L 5-HT. Distribution of GAPDH was observed with confocal microscope (H, n = 25 per group, 3 independent experiments). Scale bars, 2 μm. Western blotting was performed to assess cytoplastic and nuclear expression of GAPDH (I, n = 1 per group, 3 independent experiments).
(J) EL4 cells were transfected with mCherry-fused lentiviruses expressing either WT-GAPDH or Gln to Ala (Q46A, Q76A, Q183A, Q202A, and Q262A) mutated GAPDH. Cells were activated for 24 h, with or without 100 μmol/L 5-HT. GAPDH activity was detected (n = 5 per group, 2 independent experiments).
(K and L) WT-GAPDH or Q262A-GAPDH-transfected EL4 cells were activated for 24 h, with or without 100 μmol/L 5-HT. Distribution of GAPDH was observed with confocal microscope (K, n = 25 per group, 3 independent experiments). Scale bars, 2 μm. Western blotting was performed to assess cytoplastic and nuclear expression of mCherry-GAPDH fusion protein (L, n = 1 per group, 3 independent experiments).
(M) WT-GAPDH or Q262A-GAPDH-transfected EL4 cells were activated for 24 h, with or without 100 μmol/L 5-HT. ECAR was detected (n = 6 per group, 3 independent experiments).
(N) WT-GAPDH or Q262A-GAPDH-transfected EL4 cells were activated for 24 h, with or without 100 μmol/L 5-HT. mCherry-bonded proteins were immunoprecipitated, and chromosome region maintenance 1 (CRM1) was detected (n = 1 per group, 3 independent experiments). IP, immunoprecipitation.
Bars represent mean ± standard deviation.
See also Figure S3.

Please cite this article in press as: Wang et al., A GAPDH serotonylation system couples CD8+ T cell glycolytic metabolism to antitumor immunity, Molecular Cell (2023), https://doi.org/10.1016/j.molcel.2023.12.015

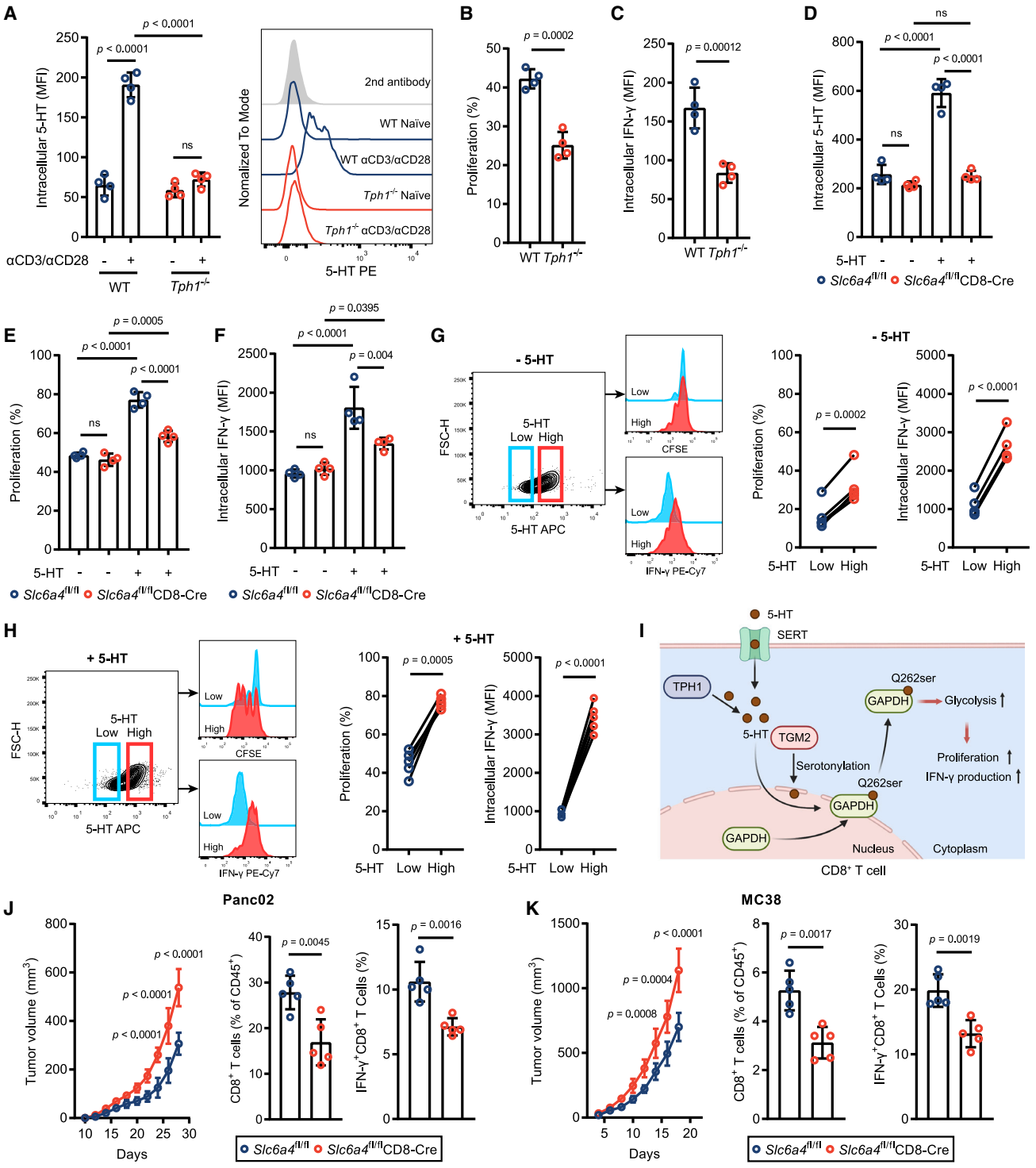

Figure 4. Intracellular accumulation of 5-HT is essential for enhancing CD8+ T cell activation and antitumor immunity

(A) WT or *Tph1*$^{-/-}$ CD8+ T cells were activated for 24 h. Intracellular 5-HT was determined (n = 4 per group, 3 independent experiments).

(B and C) WT or *Tph1*$^{-/-}$ CD8+ T cells were activated for 72 h. Cell proliferation (B) and intracellular IFN-γ (C) were determined (n = 4 per group, 3 independent experiments).

(D–F) *Slc6a4*$^{fl/fl}$ or *Slc6a4*$^{fl/fl}$CD8-Cre CD8+ T cells were activated for 24 h, with or without 100 μmol/L 5-HT. Intracellular 5-HT (D), cell proliferation (E), and intracellular IFN-γ (F) were detected (n = 4 per group, 3 independent experiments).

(legend continued on next page)

Please cite this article in press as: Wang et al., A GAPDH serotonylation system couples CD8+ T cell glycolytic metabolism to antitumor immunity, Molecular Cell (2023), https://doi.org/10.1016/j.molcel.2023.12.015

Intracellular accumulation of 5-HT is essential for enhancing CD8+ T cell activation and antitumor immunity

Different from receptor-dependent cell activation, serotonylation reaction needs accumulation of intracellular 5-HT. According to the RNA-seq and real-time qPCR results, we noticed that naïve CD8+ T cells barely expressed 5-HT synthetase *Tph1* or *Tph2*, whereas *Tph1* expression was increased in activated CD8+ T cells (Figures S4A and S4B). In addition, mRNA evidence also showed that monoamine transporter *Slc6a4* (encoding SERT) but not *Slc6a2* (norepinephrine transporter) or *Slc6a3* (encoding dopamine transporter) was found to be abundantly expressed in CD8+ T cells (Figures S4C and S4D), which was further validated by flow cytometry analyses (Figure S4E). It indicates that both endogenous production of 5-HT by TPH1 and exogenous uptake of 5-HT via SERT may contribute to the accumulation of intracellular 5-HT in CD8+ T cells. To address this issue, we first adopted TPH1-depleted *Tph1*$^{-/-}$ CD8+ T cells, and flow cytometry and ELISA analyses revealed that intracellular 5-HT accumulated in activated WT CD8+ T cells but not in *Tph1*$^{-/-}$ CD8+ T cells (Figures 4A and S4F). In addition, compared with WT CD8+ T cells, cell proliferation and IFN-γ content were significantly reduced in *Tph1*$^{-/-}$ CD8+ T cells (Figures 4B and 4C). It supports that TPH1-generated endogenous 5-HT can promote CD8+ T cell activation. Next, CD8+ T cell-specific deletion of 5-HT transporter SERT (*Slc6a4*$^{flox/flox}$*Cd8a*^{cre}, *Slc6a4*$^{fl/fl}$CD8-Cre) mice were engineered. We found that compared with *Slc6a4*$^{fl/fl}$ CD8+ T cells, SERT-deficient *Slc6a4*$^{fl/fl}$CD8-Cre CD8+ T cells blocked the uptake of 5-HT (Figures 4D and S4G). Moreover, functional studies showed that SERT deficiency suppressed the 5-HT-enhanced CD8+ T cell proliferation and IFN-γ production (Figures 4E and 4F). These observations suggest that SERT-induced uptake of 5-HT contributes to the activation of CD8+ T cells.

To further verify the involvement of intracellular 5-HT in CD8+ T cell activation, we co-stained intracellular 5-HT with carboxyfluorescein succinimidyl ester (CFSE) and IFN-γ in activated CD8+ T cells. We observed that cells with higher expression of intracellular 5-HT had an increased proliferation rate and elevated IFN-γ content (Figure 4G). 5-HT stimulation further increased the accumulation of intracellular 5-HT, and the proliferation rate and IFN-γ content were also elevated in the cells with higher 5-HT expression (Figure 4H). It supports that intracellular accumulation of endogenous and exogenous 5-HT facilitates the activation of CD8+ T cells (Figure 4I).

Tumor microenvironment is enriched with 5-HT due to the secretion of 5-HT from tumor cells[3] and the existence of platelets, which were the major 5-HT sources.[5] Therefore, we investigated the role of SERT-induced CD8+ T cell 5-HT uptake in antitumor immune activity. Panc02 and MC38 tumor cells were subcutaneously implanted into CD8+ T cell-specific SERT-depleted *Slc6a4*$^{fl/fl}$CD8-Cre mice and control *Slc6a4*$^{fl/fl}$ mice. Tumor growth was evaluated, and we observed that tumors grew faster in SERT-depleted *Slc6a4*$^{fl/fl}$CD8-Cre mice (Figures 4J and 4K). In addition, infiltration of CD8+ T cells (Figures 4J, 4K, S4H, and S4I) and intracellular IFN-γ expression were reduced in tumor-infiltrated SERT-deficient CD8+ T cells (Figures 4J, 4K, S4J, and S4K). These results indicated that intracellular 5-HT is essential for the antitumor responses of CD8+ T cells.

5-HT-induced serotonylation of GAPDH sustains the prolonged activation of CD8+ T cells

5-HT exerts its diverse biological functions through canonical 5-HTR signaling and the recently identified serotonylation post-translational modification. 5-HT was reported to regulate CD8+ T cell activation via 5-HTRs.[6] We noticed that TGM2-deficient (Figures 2H and 2I) and SERT-deficient (Figures 4E and 4F) CD8+ T cells remained partly responsive to 5-HT stimulation, indicating the potential involvement of 5-HTRs. 5-HTRs consist of 7 families and at least 15 different HTRs. We screened the expression of 5-HTRs in the RNA-seq results and found that most *Htr*s could hardly be detected in naïve or activated CD8+ T cells, except for *Htr1b* and *Htr7* (Figure 5A). Real-time qPCR (Figure S5A) and flow cytometry (Figure 5B) further verified the expression of HTR1B and HTR7 in CD8+ T cells, with upregulated expression of HTR1B and downregulated expression of HTR7 after activation. To evaluate the involvement of 5-HTRs in CD8+ T cell activation, specific agonists of HTR1B and HTR7 were used. We observed that the HTR7 agonist but not the HTR1B agonist promoted CD8+ T cell activation, but the extent was less apparent than that of 5-HT (Figure 5C). In 5-HT-stimulated CD8+ T cells, specific antagonists were adopted to block HTR1B and HTR7. The results showed that the antagonist of HTR7 but not HTR1B partially reversed 5-HT-enhanced CD8+ T cell activation (Figure 5D). The evidence from chemical agonists and antagonists indicates that HTR7 contributes to 5-HTR-induced CD8+ T cell activation.

We noticed that the expression of *Htr7* was reduced after αCD3/αCD28 activation for 1 day (Figures 5A and S5A). When the stimulation time was prolonged to 3 and 5 days, the expression of *Htr7* was further reduced (Figure 5E). We next assessed whether the decreased expression of *Htr7* could lead to decreased receptor activity. HTR7 belongs to the G-protein coupled receptors (GPCRs), and calcium ion (Ca^{2+}) serves as a second messenger.[22] An HTR7 agonist was used to stimulate naïve CD8+ T cells (day 0), or αCD3/αCD28-activated cells at days 1, 3, and 5 (Figure 5F). Intracellular Ca^{2+} flux analyses showed that the HTR7 agonist induced rapid and robust Ca^{2+}

(G and H) CD8+ T cells were activated for 72 h, with (G) or without (H) 100 μmol/L 5-HT. Intracellular 5-HT was co-stained with CFSE and IFN-γ. Cellular proliferation and IFN-γ were analyzed based on the expression of 5-HT (n = 5 per group, 3 independent experiments).

(I) Schematics showing that intracellular accumulation of 5-HT induces GAPDH Q262ser serotonylation in CD8+ T cells.

(J and K) Panc02 (J) or MC38 (K) cells were subcutaneously implanted into syngeneic *Slc6a4*$^{fl/fl}$ or *Slc6a4*$^{fl/fl}$CD8-Cre mice. Tumor volume was monitored every 2 days (n = 7 per group, 3 independent experiments). Frequency and intracellular IFN-γ of CD8+ T cells were detected (n = 5 per group, 3 independent experiments).

Bars represent mean ± standard deviation. ns indicates not significant.

See also Figure S4.

A

	Naïve			αCD3/αCD28		
Htr1a	0.00	0.00	0.00	0.00	0.00	0.00
Htr1b	0.06	0.00	0.00	0.34	0.25	0.36
Htr1d	0.00	0.02	0.00	0.00	0.00	0.00
Htr1f	0.00	0.00	0.00	0.00	0.00	0.00
Htr2a	0.03	0.13	0.00	0.00	0.00	0.02
Htr2b	0.00	0.00	0.00	0.00	0.00	0.00
Htr2c	0.00	0.00	0.00	0.00	0.00	0.00
Htr3a	0.00	0.00	0.00	0.00	0.00	0.00
Htr3b	0.00	0.00	0.00	0.00	0.00	0.00
Htr4	0.00	0.00	0.00	0.00	0.00	0.00
Htr5a	0.00	0.00	0.00	0.00	0.00	0.00
Htr5b	0.00	0.00	0.00	0.00	0.00	0.00
Htr6	0.00	0.02	0.00	0.00	0.00	0.00
Htr7	0.50	0.27	0.16	0.06	0.03	0.05

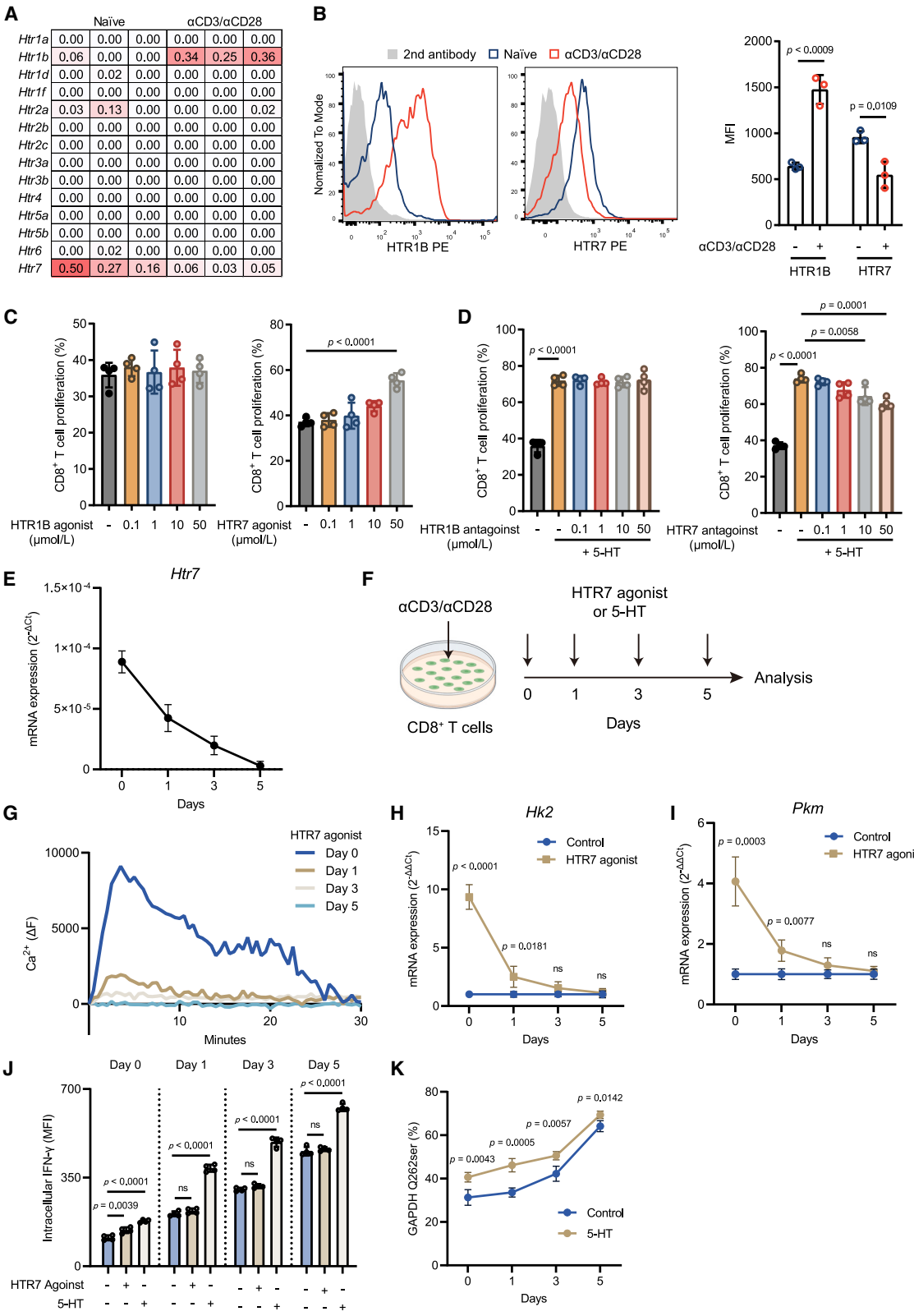

(legend on next page)

Please cite this article in press as: Wang et al., A GAPDH serotonylation system couples CD8+ T cell glycolytic metabolism to antitumor immunity, Molecular Cell (2023), https://doi.org/10.1016/j.molcel.2023.12.015

flux in naïve CD8+ T cells (Figure 5G). However, when an HTR7 agonist was used to stimulate CD8+ T cells after αCD3/αCD28 activation for 1 day, Ca^{2+} flux was impaired, and it was abolished on day 3 and day 5 (Figure 5G). Ca^{2+} flux was previously shown to promote CD8+ T cell activation by upregulating the expression of glycolysis-associated genes.[23] We found that the HTR7 agonist could promoted the expression of *Hk2* and *Pkm* (Figures 5H and 5I). However, with prolonged culture time, the upregulated expression of *Hk2* and *Pkm* was abolished (Figures 5H and 5I). Intracellular IFN-γ analyses also showed that HTR7-induced activation of CD8+ T cells was diminished over time (Figures 5J and S5B). However, this finding was inconsistent with the results showing that 5-HT could still promote CD8+ T cell activation on day 5 (Figures 5J and S5B). Interestingly, by detecting GAPDH serotonylation, we observed that 5-HT-induced GAPDH serotonylation was still evidently upregulated in the prolonged activation time (Figures 5K and S5C). This indicates that GAPDH serotonylation but not HTR7 sustains long-term activation of CD8+ T cells.

MAOA degrades intracellular 5-HT and inhibits the antitumor activity of CD8+ T cells by restraining GAPDH serotonylation

Monoamine oxidases, including MAOA and MAOB, serve to catabolize monoamine neurotransmitters, including 5-HT.[24] We observed that *Maoa* was expressed in naïve CD8+ T cells, and after activation, *Maoa* expression was further upregulated (Figures S6A and S6B). By contrast, *Maob* was barely detected in naïve or activated CD8+ T cells. To identify the involvement of MAOA in CD8+ T cell activation, we generated CD8+ T cell conditional MAOA knockout (*Maoa*$^{flox/flox}$*Cd8a*^{cre}, *Maoa*$^{fl/fl}$CD8-Cre) mice. Compared with *Maoa*$^{fl/fl}$ CD8+ T cells, *Maoa*$^{fl/fl}$CD8-Cre CD8+ T cells had increased intracellular 5-HT content (Figures 6A and S6C). Glycolytic metabolism, as indicated by GAPDH activity and ECAR, was enhanced in MAOA-deficient cells (Figures 6B, 6C, and S6D). The cytoplasmic localization of GAPDH was also reinforced in MAOA-deficient CD8+ T cells (Figures 6D, 6E, S6E, and S6F). Functional analyses showed that cell proliferation and IFN-γ production were elevated in MAOA-deficient CD8+ T cells in the presence or absence of exogenous 5-HT (Figures 6F and 6G). Immunoblotting studies confirmed that serotonylation of GAPDH Q262ser was enhanced in MAOA-deficient cells (Figures 6H and S6G). A TGM2 inhibitor was used to treat CD8+ T cells, and we found that GAPDH activity was impaired (Figure S6H). In addition, activation of *Maoa*$^{fl/fl}$CD8-Cre CD8+ T cells was reduced to a level similar to that of *Maoa*$^{fl/fl}$ CD8+ T cells (Figure S6I), indicating that MAOA-induced CD8+ T cell activation was associated with TGM2-involved GAPDH serotonylation.

To determine whether MAOA can inhibit CD8+ T cell antitumor immunity *in vivo*, Panc02 and MC38 tumor cells were injected subcutaneously into syngeneic *Maoa*$^{fl/fl}$ and *Maoa*$^{fl/fl}$CD8-Cre mice. The results showed that tumor growth was inhibited in MAOA-deficient *Maoa*$^{fl/fl}$CD8-Cre mice compared with that in *Maoa*$^{fl/fl}$ mice (Figures 6I and 6J). The number of intratumoral CD8+ T cells was increased in MAOA-deficient *Maoa*$^{fl/fl}$CD8-Cre mice (Figures 6I, 6J, S6J, and S6K). Moreover, tumor-infiltrated MAOA-depleted CD8+ T cells expressed more IFN-γ than MAOA-complete CD8+ T cells (Figures 6I, 6J, S6L, and S6M). These observations from *in vitro* and *in vivo* support that MAOA restrains the antitumor activity of CD8+ T cells by reducing intracellular 5-HT and suppressing GAPDH serotonylation.

Overexpression of TPH1 in CAR-T cells to produce 5-HT improves antitumor efficacy

To evaluate the therapeutic potential of CD8+ T cell serotonylation in tumor immunotherapy, we investigated its role in the antitumor efficacy of chimeric antigen receptor T (CAR-T) cells. T cells were transduced with a CAR targeting human epidermal growth factor receptor variant III (EGFRvIII), and a cassette encoding TPH1 was inserted (Figure 7A). Efficient transduction was validated by F(ab′)$_2$ staining (Figure S7A), and upregulated TPH1 expression was examined by real-time qPCR (Figure S7B). We observed that TPH1-overexpressing CAR-T (TPH1-CAR-T) cells had increased level of intracellular 5-HT (Figure 7B). Western blotting analysis confirmed that the expression of GAPDH Q262ser was upregulated in TPH1-CAR-T cells (Figures 7C and S7C). By counting cell numbers after CAR transduction, increased cell proliferation was indicated in TPH1-CAR-T cells (Figure 7D). MC38 cells were engineered to express EGFRvIII and applied as the target cells. *In vitro* coculture antigen-specific

Figure 5. 5-HT-induced serotonylation of GAPDH sustains the prolonged activation of CD8+ T cells

(A and B) CD8+ T cells were activated for 24 h. 5-HT receptor mRNA expression was analyzed by RNA sequencing (A, n = 3 per group, 1 independent experiment). Cell membrane HTR1B and HTR7 expressions were detected by flow cytometry (B, n = 3 per group, 2 independent experiments).

(C and D) CD8+ T cells were activated for 72 h, with or without agonists (C) or antagonists (D) of HTR1B and HTR7. Cell proliferation was detected (n = 4 per group, 3 independent experiments).

(E) CD8+ T cells were activated for 0, 1, 3, and 5 days. *Htr7* mRNA expression was analyzed (n = 4 per group, 3 independent experiments).

(F) Schematic showing that αCD3/αCD28-activated CD8+ T cells were stimulated with HTR7 agonist or 5-HT at indicated times.

(G) CD8+ T cells were activated for 1, 3, and 5 days. HTR7 agonist AS-19 (50 μmol/L) was used to treat the cells, and Ca^{2+} flux was assessed (n = 3 per group, 3 independent experiments).

(H and I) CD8+ T cells were activated for 1, 3, and 5 days. HTR7 agonist (50 μmol/L) was used to treat the cells for an additional 1 day. mRNA expression of *Hk2* (H) and *Pkm* (I) was detected (n = 4 per group, 3 independent experiments).

(J) CD8+ T cells were activated for 1, 3, and 5 days. 5-HT (100 μmol/L) or HTR7 agonist (50 μmol/L) was used to treat the cells for an additional 1 day. Intracellular IFN-γ was assessed (n = 4 per group, 3 independent experiments).

(K) CD8+ T cells were activated for 1, 3, and 5 days. 5-HT (100 μmol/L) was used to treat the cells for an additional 1 day. Expression of GAPDH Q262ser was assessed (n = 4 per group, 3 independent experiments).

Bars represent mean ± standard deviation. ns indicates not significant.

See also Figure S5.

Please cite this article in press as: Wang et al., A GAPDH serotonylation system couples CD8+ T cell glycolytic metabolism to antitumor immunity, Molecular Cell (2023), https://doi.org/10.1016/j.molcel.2023.12.015

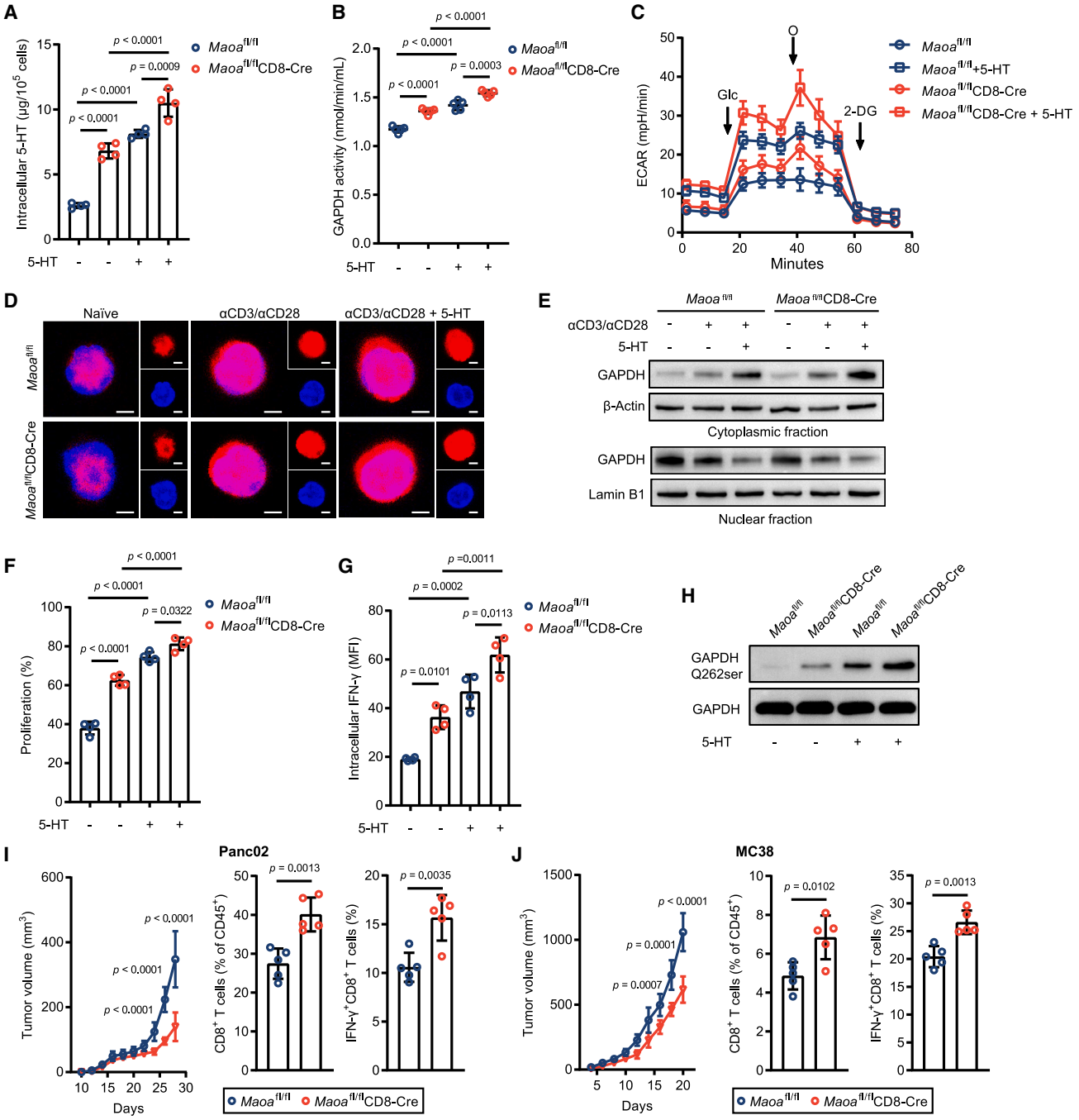

Figure 6. MAOA degrades intracellular 5-HT and inhibits the antitumor activity of CD8+ T cells by restraining GAPDH serotonylation

(A–C) *Maoa*$^{fl/fl}$ or *Maoa*$^{fl/fl}$CD8-Cre CD8+ T cells were activated for 24 h, with or without 100 μmol/L 5-HT. Intracellular 5-HT (A, n = 4 per group, 3 independent experiments), GAPDH activity (B, n = 5 per group, 2 independent experiments), and ECAR (C, n = 4 per group, 3 independent experiments) were detected.

(D and E) *Maoa*$^{fl/fl}$ or *Maoa*$^{fl/fl}$CD8-Cre CD8+ T cells were activated for 24 h, with or without 100 μmol/L 5-HT. Distribution of GAPDH was observed with confocal microscope (D, n = 25 per group, 3 independent experiments). Scale bars, 2 μm. Western blotting was performed to assess cytoplastic and nuclear expression of GAPDH (E, n = 1 per group, 3 independent experiments).

(F and G) *Maoa*$^{fl/fl}$ or *Maoa*$^{fl/fl}$CD8-Cre CD8+ T cells were activated for 72 h, with or without 100 μmol/L 5-HT. Cell proliferation (F) and intracellular IFN-γ (G) were detected (n = 4 per group, 2 independent experiments).

(H) *Maoa*$^{fl/fl}$ or *Maoa*$^{fl/fl}$CD8-Cre CD8+ T cells were activated for 24 h, with or without 100 μmol/L 5-HT. Serotonylation of GAPDH Q262ser was analyzed (n = 1 per group, 3 independent experiments).

(legend continued on next page)

Please cite this article in press as: Wang et al., A GAPDH serotonylation system couples CD8+ T cell glycolytic metabolism to antitumor immunity, Molecular Cell (2023), https://doi.org/10.1016/j.molcel.2023.12.015

cytotoxicity analysis showed that TPH1-CAR-T cells had enhanced antitumor activity (Figure 7E). In addition, TPH1-CAR-T cells released more IFN-γ than CAR-T cells when cocultured with target tumor cells (Figure 7F). To further assess the *in vivo* antitumor effects, EGFRvIII-expressing MC38 cells were implanted into syngeneic C57BL/6 mice. 5 days after inoculation, EGFRvIII-specific CAR-T cells or TPH1-CAR-T cells were transferred to the tumor-bearing mice. Compared with the non-CAR-T cell-transferred group, EGFRvIII-specific CAR-T cells significantly inhibited tumor growth, and tumor volume was reduced to approximately 68% at 23 days (Figure 7G). Transfer of TPH1-CAR-T cells further reduced the tumor growth, and tumor volume was reduced to approximately 22% at 23 days (Figure 7G). The enhanced antitumor activity of TPH1-CAR-T cells was further confirmed by immunohistochemical staining for Ki67 and cleaved caspase-3 (Figure 7H). Therefore, these data support the therapeutic potential of 5-HT-producing TPH1-CAR-T cells in tumor immunotherapy.

DISCUSSION

Hexokinase, phosphofructokinase, and pyruvate kinase are recognized as the three canonical rate-limiting enzymes in glycolysis. Recent evidence has revealed that GAPDH becomes a rate-limiting enzyme in cells that utilize aerobic glycolysis as the primary energic source.[25,26] The metabolic shift to aerobic glycolysis is a hallmark of the activation of effector CD8+ T cells, which suggests that the manipulation of GAPDH enzymatic activity is essential for enhancing CD8+ T cell glycolytic metabolism and activation. Here, we identified serotonylation as a GAPDH post-translational modification that promotes GAPDH glycolytic activity. Previous studies have proven that cytoplasmic GAPDH possesses higher glycolytic activity than nuclear GAPDH,[20] and upregulated expression of cytoplastic GAPDH enhances CD8+ T cell glycolytic metabolism of and promotes their activation.[21] However, the molecular event that underlies the subcellular localization of GAPDH is elusive. GAPDH lacks an NLS,[19] but intriguingly contains an NES.[17] Post-translational modification is crucial for GAPDH nuclear-cytoplasmic trafficking. S-nitrosylation of cysteine 150,[19] phosphorylation of threonine 237,[27] phosphorylation of serine 234,[28] and acetylation of lysine 217[29] were reported to mediate the nuclear-cytoplasmic transport of GAPDH. However, none of these amino acid residues reside in the NES of GAPDH. Our findings revealed that Q262 at the GAPDH NES could be serotonylated. Given that GAPDH Q262 and the known post-translational sites are separated by dozens of amino acids, the direct interaction between them seems impractical. The exportin CRM1 was reported to export the GAPDH protein by interacting with the NES sequence.[17] We found that GAPDH Q262ser serotonylation promoted the interaction between GAPDH and CRM1, which contributed to the nuclear-cytoplasmic trafficking of GAPDH. This result provides compelling evidence that post-translational modification of GAPDH NES is essential for regulating its subcellular localization.

Serotonylation post-translational modification has been shown to occur in various different proteins. H3Q5ser serotonylation was recently identified as a permissive post-translational modification that coexists with adjacent H3K4me3 and regulates neuron differentiation.[8,30] In addition, the authors identified that H3K4me3Q5ser serotonylation was expressed in almost all organs, and robust expression was observed in peripheral circulating leukocytes.[8] H3K4me is a marker of active transcription, which plays important roles in cell differentiation, organism longevity, metabolism, and cancer development.[31] Our study showed that histone H3 was the substrate for serotonylation in CD8+ T cells (Figure 1F). Whether H3K4me3Q5ser serotonylation can mediate the function of CD8+ T cells remains unknown, and it will be particularly interesting for further explorations.

Although CAR-T cell therapy has achieved encouraging results in hematological tumors, clinical data of CAR-T cell therapy in solid tumors are disappointing.[32] Novel strategies are needed to improve the antitumor activity of CAR-T cells in the tumor microenvironment.[32] We found that overexpression of TPH1 in CAR-T cells to produce 5-HT resulted in enhanced GAPDH Q262ser serotonylation and improved control of tumor growth, providing a promising target for further investigations in human CAR-T cells.

Limitations of the study

Previous reports have shown that serotonylation modification occurred in various different proteins. Our data of LC-MS/MS data revealed that hundreds of proteins may be serotonylated in CD8+ T cells. We cannot exclude the possibility that other serotonylated protein(s) may also be associated with the activation of CD8+ T cells. mCherry was used to label WT or mutated GAPDH in EL4 cells. A recent publication revealed that the mCherry sequence has an alternative start codon that generates splice variants, and this may potentially interfere with the localization assay.[33] Finally, our observations are derived from murine models. Although the NES sequence of GAPDH is conserved in humans and mice, samples from human tumor-infiltrated CD8+ T cells may help to develop the clinical relevance of GAPDH Q262ser modification in tumor immune responses.

STAR★METHODS

Detailed methods are provided in the online version of this paper and include the following:

- KEY RESOURCES TABLE
- RESOURCE AVAILABILITY
  - Lead contact
  - Materials availability

(I and J) Panc02 (I) or MC38 (J) cells were subcutaneously implanted into syngeneic *Maoa*$^{fl/fl}$ or *Maoa*$^{fl/fl}$CD8-Cre mice. Tumor volume was monitored every 2 days (n = 7 per group, 3 independent experiments). Frequency and intracellular IFN-γ of CD8+ T cells were detected (n = 5 per group, 2 independent experiments). Bars represent mean ± standard deviation. ns indicates not significant.
See also Figure S6.

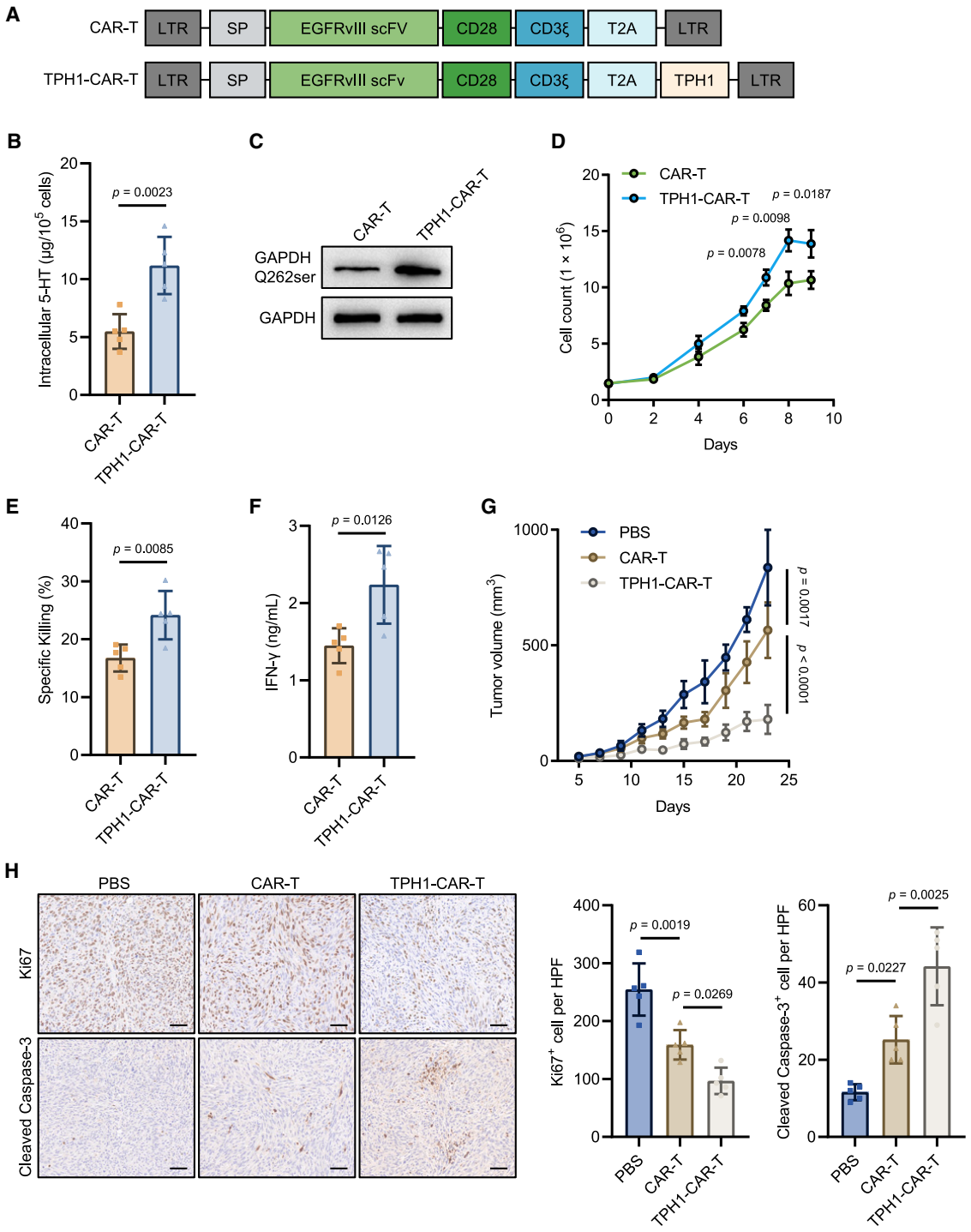

Figure 7. Overexpression of TPH1 in CAR-T cells to produce 5-HT improves antitumor efficacy

(A) Schematic showing the domain organization of CAR construct. LTR, long terminal repeat; SP, signal peptide; scFv, single-chain variable fragment; T2A, T2A sequence.

(B) Intracellular 5-HT was detected in CAR-T and TPH1-CAR-T cells (n = 5 per group, 3 independent experiments).

(C) Expression of GAPDH Q262ser was detected in CAR-T and TPH1-CAR-T cells (n = 1 per group, 3 independent experiments).

(D) Cell numbers of CAR-T cells and TPH1-CAR-T cells were counted after retrovirus transduction (n = 3 per group, 3 independent experiments).

(E and F) CAR-T or TPH1-CAR-T cells were cocultured with EGFPvIII-expressed MC38 cells for 24 h. Cell vitality (E) and IFN-γ (F) release were detected (n = 5 per group, 3 independent experiments).

(legend continued on next page)

SUPPLEMENTAL INFORMATION

Supplemental information can be found online at https://doi.org/10.1016/j.molcel.2023.12.015.

ACKNOWLEDGMENTS

This study was supported by the National Natural Science Foundation of China (ID 32170910 to X.W.; 82230087, 82350123, and 92168111 to Z.-G.Z.), the Natural Science Foundation of Jiangsu Province (BK20211124 to X.W.), the Natural Science Foundation of Shanghai (22ZR1460000 to X.-L.Z.), the Shanghai Municipal Education Commission Gaofeng Clinical Medicine Grant Support (20181708 to Z.-G.Z.), the Medicine and Engineering Interdisciplinary Research Fund of Shanghai Jiao Tong University (YG2021ZD08 to Z.-G.Z.), the Innovative Research Team of High-Level Local Universities in Shanghai (SHSMU-ZDCX20210802 to Z.-G.Z.), the Shanghai Pilot Program for Basic Research-Shanghai Jiao Tong University (21TQ1400225 to Z.-G.Z.), the 111 Project (number B21024 to Z.-G.Z.), the Zhenjiang Key Research and Development Program (SH2021037 to X.W.), and the Postgraduate Research & Practice Innovation Program of Jiangsu Province (5561280087 to S.-Q.F.).

AUTHOR CONTRIBUTIONS

Z.-G.Z. conceived the project. X.-L.Z., L.-P.H., S.-H.J., and X.Z. designed experiments and interpreted the data in the manuscript. X.W. performed statistical analysis and wrote the manuscript. X.W., Q.J., S.-Q.F., R.-K.L., and X.Y. performed animal studies. F.Y. and H.-W.T. prepared CAR-T cells. S.H., Y.Y., S.-Y.X., A.T., and P.-Q.H. performed immunoprecipitation and western blotting analyses. W.-T.Q., H.Z., C.D., H.-W.T., X.-F.W., L.-L.Y., and J.L. conducted CD8+ T cell functional studies. D.-X.L. and C.-H.D. helped perform statistical analysis. H.L. performed bioinformatics analyses. X.W., S.-Q.F., X.Y., F.Y., Q.J., and H.-W.T. were equal in significance to the final conclusions of the study; therefore, the authorship order reflects their temporal involvement in the project.

DECLARATION OF INTERESTS

The authors declare no competing interests.

Received: March 6, 2023
Revised: October 4, 2023
Accepted: December 12, 2023
Published: January 11, 2024

REFERENCES

1. Spohn, S.N., and Mawe, G.M. (2017). Non-conventional features of peripheral serotonin signalling - the gut and beyond. Nat. Rev. Gastroenterol. Hepatol. *14*, 412–420.
2. Crane, J.D., Palanivel, R., Mottillo, E.P., Bujak, A.L., Wang, H., Ford, R.J., Collins, A., Blümer, R.M., Fullerton, M.D., Yabut, J.M., et al. (2015). Inhibiting peripheral serotonin synthesis reduces obesity and metabolic dysfunction by promoting brown adipose tissue thermogenesis. Nat. Med. *21*, 166–172.
3. Jiang, S.H., Li, J., Dong, F.Y., Yang, J.Y., Liu, D.J., Yang, X.M., Wang, Y.H., Yang, M.W., Fu, X.L., Zhang, X.X., et al. (2017). Increased serotonin signaling contributes to the Warburg effect in pancreatic tumor cells under metabolic stress and promotes growth of pancreatic tumors in mice. Gastroenterology *153*, 277–291.e19.
4. Zhu, P., Lu, T., Chen, Z., Liu, B., Fan, D., Li, C., Wu, J., He, L., Zhu, X., Du, Y., et al. (2022). 5-hydroxytryptamine produced by enteric serotonergic neurons initiates colorectal cancer stem cell self-renewal and tumorigenesis. Neuron *110*, 2268–2282.e4.
5. Schneider, M.A., Heeb, L., Beffinger, M.M., Pantelyushin, S., Linecker, M., Roth, L., Lehmann, K., Ungethüm, U., Kobold, S., Graf, R., et al. (2021). Attenuation of peripheral serotonin inhibits tumor growth and enhances immune checkpoint blockade therapy in murine tumor models. Sci. Transl. Med. *13*, eabc8188.
6. Wang, X., Li, B., Kim, Y.J., Wang, Y.C., Li, Z., Yu, J., Zeng, S., Ma, X., Choi, I.Y., Di Biase, S., et al. (2021). Targeting monoamine oxidase A for T cell-based cancer immunotherapy. Sci. Immunol. *6*, eabh2383.
7. Walther, D.J., Peter, J.U., Winter, S., Höltje, M., Paulmann, N., Grohmann, M., Vowinckel, J., Alamo-Bethencourt, V., Wilhelm, C.S., Ahnert-Hilger, G., and Bader, M. (2003). Serotonylation of small GTPases is a signal transduction pathway that triggers platelet alpha-granule release. Cell *115*, 851–862.
8. Farrelly, L.A., Thompson, R.E., Zhao, S., Lepack, A.E., Lyu, Y., Bhanu, N.V., Zhang, B., Loh, Y.E., Ramakrishnan, A., Vadodaria, K.C., et al. (2019). Histone serotonylation is a permissive modification that enhances TFIID binding to H3K4me3. Nature *567*, 535–539.
9. Jiang, S.H., Wang, Y.H., Hu, L.P., Wang, X., Li, J., Zhang, X.L., and Zhang, Z.G. (2021). The physiology, pathology and potential therapeutic application of serotonylation. J. Cell Sci. *134*.
10. Sima, L.E., Chen, S., Cardenas, H., Zhao, G., Wang, Y., Ivan, C., Huang, H., Zhang, B., and Matei, D. (2021). Loss of host tissue transglutaminase

(G) EGFRvIII-expressing MC38 cells were subcutaneously implanted into syngeneic C57BL/6 mice. CAR-T or TPH1-CAR-T cells were adoptively transferred at day 5. Tumor volume was monitored every 2 days (n = 7 per group, 2 independent experiments).
(H) Ki67 and cleaved caspase-3 were detected in CAR-T and TPH1-CAR-T cells transferred mice (n = 5 per group, 2 independent experiments). Scale bars, 50 μm.
Bars represent mean ± standard deviation.
See also Figure S7.

boosts antitumor T cell immunity by altering STAT1/STAT3 phosphorylation in ovarian cancer. J. Immunother. Cancer *9*, jcs257337.

11. De Giovanni, M., Tam, H., Valet, C., Xu, Y., Looney, M.R., and Cyster, J.G. (2022). GPR35 promotes neutrophil recruitment in response to serotonin metabolite 5-HIAA. Cell *185*, 1103–1104.
12. Møller, S.H., Hsueh, P.C., Yu, Y.R., Zhang, L., and Ho, P.C. (2022). Metabolic programs tailor T cell immunity in viral infection, cancer, and aging. Cell Metab. *34*, 378–395.
13. Watts, S.W., Priestley, J.R., and Thompson, J.M. (2009). Serotonylation of vascular proteins important to contraction. PLoS One *4*, e5682.
14. Penumatsa, K.C., Toksoz, D., Warburton, R.R., Kharnaf, M., Preston, I.R., Kapur, N.K., Khosla, C., Hill, N.S., and Fanburg, B.L. (2017). Transglutaminase 2 in pulmonary and cardiac tissue remodeling in experimental pulmonary hypertension. Am. J. Physiol. Lung Cell. Mol. Physiol. *313*, L752–L762.
15. Ivashkin, E., Melnikova, V., Kurtova, A., Brun, N.R., Obukhova, A., Khabarova, M.Y., Yakusheff, A., Adameyko, I., Gribble, K.E., and Voronezhskaya, E.E. (2019). Transglutaminase activity determines nuclear localization of serotonin immunoreactivity in the early embryos of invertebrates and vertebrates. ACS Chem. Neurosci. *10*, 3888–3899.
16. Hummerich, R., Costina, V., Findeisen, P., and Schloss, P. (2015). Monoaminylation of fibrinogen and glia-derived proteins: indication for similar mechanisms in posttranslational protein modification in blood and brain. ACS Chem. Neurosci. *6*, 1130–1136.
17. Brown, V.M., Krynetski, E.Y., Krynetskaia, N.F., Grieger, D., Mukatira, S.T., Murti, K.G., Slaughter, C.A., Park, H.W., and Evans, W.E. (2004). A novel CRM1-mediated nuclear export signal governs nuclear accumulation of glyceraldehyde-3-phosphate dehydrogenase following genotoxic stress. J. Biol. Chem. *279*, 5984–5992.
18. Zhang, H., Zhao, Y., and Zhou, D.X. (2017). Rice NAD^+-dependent histone deacetylase OsSRT1 represses glycolysis and regulates the moonlighting function of GAPDH as a transcriptional activator of glycolytic genes. Nucleic Acids Res. *45*, 12241–12255.
19. Hara, M.R., Agrawal, N., Kim, S.F., Cascio, M.B., Fujimuro, M., Ozeki, Y., Takahashi, M., Cheah, J.H., Tankou, S.K., Hester, L.D., et al. (2005). S-nitrosylated GAPDH initiates apoptotic cell death by nuclear translocation following Siah1 binding. Nat. Cell Biol. *7*, 665–674.
20. Mazzola, J.L., and Sirover, M.A. (2003). Subcellular localization of human glyceraldehyde-3-phosphate dehydrogenase is independent of its glycolytic function. Biochim. Biophys. Acta *1622*, 50–56.
21. Gubser, P.M., Bantug, G.R., Razik, L., Fischer, M., Dimeloe, S., Hoenger, G., Durovic, B., Jauch, A., and Hess, C. (2013). Rapid effector function of memory CD8+ T cells requires an immediate-early glycolytic switch. Nat. Immunol. *14*, 1064–1072.
22. Morita, T., McClain, S.P., Batia, L.M., Pellegrino, M., Wilson, S.R., Kienzler, M.A., Lyman, K., Olsen, A.S., Wong, J.F., Stucky, C.L., et al. (2015). HTR7 mediates serotonergic acute and chronic itch. Neuron *87*, 124–138.
23. Vaeth, M., Maus, M., Klein-Hessling, S., Freinkman, E., Yang, J., Eckstein, M., Cameron, S., Turvey, S.E., Serfling, E., Berberich-Siebelt, F., et al. (2017). Store-operated Ca^{2+} entry controls clonal expansion of T cells through metabolic reprogramming. Immunity *47*, 664–679.e6.
24. Okaty, B.W., Commons, K.G., and Dymecki, S.M. (2019). Embracing diversity in the 5-HT neuronal system. Nat. Rev. Neurosci. *20*, 397–424.
25. Kornberg, M.D., Bhargava, P., Kim, P.M., Putluri, V., Snowman, A.M., Putluri, N., Calabresi, P.A., and Snyder, S.H. (2018). Dimethyl fumarate targets GAPDH and aerobic glycolysis to modulate immunity. Science *360*, 449–453.
26. Liberti, M.V., Dai, Z., Wardell, S.E., Baccile, J.A., Liu, X., Gao, X., Baldi, R., Mehrmohamadi, M., Johnson, M.O., Madhukar, N.S., et al. (2017). A predictive model for selective targeting of the Warburg effect through GAPDH inhibition with a natural product. Cell Metab. *26*, 648–659.e8.
27. Huang, Q., Lan, F., Zheng, Z., Xie, F., Han, J., Dong, L., Xie, Y., and Zheng, F. (2011). Akt2 kinase suppresses glyceraldehyde-3-phosphate dehydrogenase (GAPDH)-mediated apoptosis in ovarian cancer cells via phosphorylating GAPDH at threonine 237 and decreasing its nuclear translocation. J. Biol. Chem. *286*, 42211–42220.
28. Chang, C., Su, H., Zhang, D., Wang, Y., Shen, Q., Liu, B., Huang, R., Zhou, T., Peng, C., Wong, C.C., et al. (2015). AMPK-dependent phosphorylation of GAPDH triggers Sirt1 activation and is necessary for autophagy upon glucose starvation. Mol. Cell *60*, 930–940.
29. Balmer, M.L., Ma, E.H., Bantug, G.R., Grählert, J., Pfister, S., Glatter, T., Jauch, A., Dimeloe, S., Slack, E., Dehio, P., et al. (2016). Memory CD8(+) T cells require increased concentrations of acetate induced by stress for optimal function. Immunity *44*, 1312–1324.
30. Zhao, S., Chuh, K.N., Zhang, B., Dul, B.E., Thompson, R.E., Farrelly, L.A., Liu, X., Xu, N., Xue, Y., Roeder, R.G., et al. (2021). Histone H3Q5 serotonylation stabilizes H3K4 methylation and potentiates its readout. Proc. Natl. Acad. Sci. USA *118*, e2016742118..
31. Shilatifard, A. (2012). The COMPASS family of histone H3K4 methylases: mechanisms of regulation in development and disease pathogenesis. Annu. Rev. Biochem. *81*, 65–95.
32. Newick, K., O'Brien, S., Moon, E., and Albelda, S.M. (2017). CAR T cell therapy for solid tumors. Annu. Rev. Med. *68*, 139–152.
33. Fages-Lartaud, M., Tietze, L., Elie, F., Lale, R., and Hohmann-Marriott, M.F. (2022). mCherry contains a fluorescent protein isoform that interferes with its reporter function. Front. Bioeng. Biotechnol. *10*, 892138.
34. Lin, J.C., Chou, C.C., Gao, S., Wu, S.C., Khoo, K.H., and Lin, C.H. (2013). An in vivo tagging method reveals that Ras undergoes sustained activation upon transglutaminase-mediated protein serotonylation. Chembiochem *14*, 813–817.
35. Agliardi, G., Liuzzi, A.R., Hotblack, A., De Feo, D., Núñez, N., Stowe, C.L., Friebel, E., Nannini, F., Rindlisbacher, L., Roberts, T.A., et al. (2021). Intratumoral IL-12 delivery empowers CAR-T cell immunotherapy in a pre-clinical model of glioblastoma. Nat. Commun. *12*, 444.

Please cite this article in press as: Wang et al., A GAPDH serotonylation system couples CD8+ T cell glycolytic metabolism to antitumor immunity, Molecular Cell (2023), https://doi.org/10.1016/j.molcel.2023.12.015

STAR★METHODS

KEY RESOURCES TABLE

REAGENT or RESOURCE	SOURCE	IDENTIFIER
Antibodies		
CD8a (Ly-2) Microbeads	Miltenyi	Cat.#130-117-044
CD3ε Microbeads	Miltenyi	Cat.# 130-094-973
Ultra-LEAF Purified anti-mouse CD3ε	Biolegend	Cat.#100341; RRID: AB_2832292
Ultra-LEAF Purified anti-mouse CD28	Biolegend	Cat.#102116; RRID: AB_11150408
PE anti-human/mouse Granzyme B	Biolegend	Cat.#396406; RRID: AB_2687031
Brilliant Violet 605 anti-mouse CD8a	Biolegend	Cat.#100744; RRID: AB_2616811
PercP-Cy5.5 Rat Anti-Mouse CD45	BD Biosciences	Cat.#550994; RRID:AB_394003
FITC Rat Anti-Mouse IFN-γ	BD Biosciences	Cat.#554411; RRID: AB_395375
PE-Cy7 Rat Anti-Mouse IFN-γ	BD Biosciences	Cat.#557649; RRID: AB_396766
Anti-Serotonin	Sigma	Cat.#S5545; RRID: AB_477522
Anti-GAPDH	Abcam	Cat.#ab181602; RRID: AB_2630358
APC anti-mouse/human CD11b	Biolegend	Cat.#101211; RRID: AB_312794
APC/Cyanine7 anti-mouse Ly-6C	BD Biosciences	Cat.#560596; RRID: AB_10643867
Alexa Fluor 647 anti-mouse CD4	Biolegend	Cat.# 100426; RRID: AB_493519
PE anti-mouse CD8a	Biolegend	Cat.#100707; RRID: AB_312746
APC/Cyanine7 anti-mouse Ly-6G	Biolegend	Cat#127623; RRID: AB_10645331
Anti-IgG F(ab')$_2$ Fragment	Jackson ImmunoResearch	Cat.#115-605-006; RRID: AB_2338903
Anti-HTR1B	Alomone	Cat.#ASR-022; RRID: AB_10561260
Anti-HTR7	Alomone	Cat#ASR-037; RRID: AB_2876849
Anti-SERT	Alomone	Cat.# AMT-004; RRID: AB_10918819
Anti-Lamin B1	Proteintech	Cat.#12987-1-AP; RRID: AB_2136290
Anti-CRM1	Proteintech	Cat#27917-1-AP; RRID: AB_2881009
Anti-β-Actin	Cell Signaling Technology	Cat.#4970S; RRID: AB_2223172
Anti-mCherry	Abcam	Cat.#AB213511; RRID: AB_2814891
PE Rat Anti-Mouse CD62L	BD Biosciences	Cat.#553151; RRID: AB_39466

(*Continued on next page*)

Please cite this article in press as: Wang et al., A GAPDH serotonylation system couples CD8+ T cell glycolytic metabolism to antitumor immunity, Molecular Cell (2023), https://doi.org/10.1016/j.molcel.2023.12.015

Continued

REAGENT or RESOURCE	SOURCE	IDENTIFIER
FITC Rat Anti-Mouse CD44	BD Biosciences	Cat.#561859; RRID: AB_10894581
Anti-CD8a	Abcam	Cat.#ab217344 RRID: AB_2890649
Anti-Ki67	Abcam	Cat.#ab15580 RRID: AB_443209
Anti-cleaved Caspase-3	Cell Signaling Technology	Cat.#9661 RRID: AB_2341188
Anti-CD4	Biolegend	Cat.# 100402; RRID: AB_312687
Chemicals, peptides, and recombinant proteins		
CFSE	Invitrogen	Cat.#65-0850-84
5-HT	Sigma-Aldrich	Cat.#H9523
GAPDH	Novus Biologicals	Cat.#NBP2-52622
Fibrinogen	Sigma-Aldrich	Cat.#F4883
MDC	Sigma-Aldrich	Cat.#D4008
Cystamine	Sigma-Aldrich	Cat.#C121509
TGM2	Novus Biologicals	Cat.# 4376-TG
Biotin azide	Thermo Fisher	Cat.#B10184
Nuclear and Cytoplasmic Extraction Kit	Thermo Fisher	Cat.#78833
2-Deoxy-D-glucose	MCE	Cat.#116869
LDN-27219	MCE	Cat.#SML0744
LS Columns	Miltenyi Biotec	Cat.#130-042-401
BSA	Moregate	Cat.#BSA7TV
Heptelidic acid	Abcam	Cat.#GR-3399326
DMEM	Sigma	Cat.#D2650
EDTA	Solarbio	Cat#E1170
PBS pH7.4	BasalMedia	Cat.#B320KJ
RPMI 1640	Bioagerio	Cat.#LR1634-500
Penicillin-Streptomycin Solution 100x	Bioagerio	Cat.#XA4122
Fetal Bovine Serum	Gibco	Cat.#10099-141C
SB-224289 hydrochloride	Tocris	Cat.#180084-26-8
CP-94253 hydrochloride	Tocris	Cat.#845861-39-4
SB-258719 hydrochloride	Tocris	Cat.#1217674-10-6
AS-19	Tocris	Cat.#1000578-26-6
Critical commercial assays		
Click-iT™ Cell Reaction Buffer Kit	Thermo Fisher	Cat.#C33372
Glycolysis Stress Test Kit	Agilent	Cat.#103020
Mito Stress Test Kit	Agilent	Cat.#103015
GAPDH Activity Assay Kit	Abcam	Cat.#ab204732
Enolase Activity Assay Kit	Sigma	Cat.#MAK178
Lactate Dehydrogenase Activity Assay Kit	Sigma	Cat.#MAK066
Cytofix/Cytoperm	BD-Biosciences	Cat.#1341733
Protein G Immunoprecipitation Kit	Thermo	Cat.#10007D
PCR Kit	Takara	Cat.#R011
Fluo-4-AM	Thermo	Cat.#F14201
Cell Counting Kit-8	MCE	Cat.#HY-K0301
Deposited data		
RNA-seq data	This paper	PRJNA884743

(*Continued on next page*)

Please cite this article in press as: Wang et al., A GAPDH serotonylation system couples CD8+ T cell glycolytic metabolism to antitumor immunity, Molecular Cell (2023), https://doi.org/10.1016/j.molcel.2023.12.015

Continued

REAGENT or RESOURCE	SOURCE	IDENTIFIER
Experimental models: Cell lines		
Mouse: MC38 cells	Cell bank of Chinese Academy of Sciences	N/A
Mouse: Panc02 cells	Cell bank of Chinese Academy of Sciences	N/A
Mouse: EL4 cells	ATCC	TIB-39
Oligonucleotides		
See Table S2 for list of primers	This paper	N/A
Software and algorithms		
ImageJ	ImageJ	https://imagej.nih.gov/ij/
FlowJo	FlowJo LLC	https://www.flowjo.com/solutions/flowjo/downloads
Adobe Illustrator	Adobe Illustrator (Ai)	https://www.adobe.com/products/illustrator.html
Wave	Agilent	https://www.agilent.com/en/products/cell-analysis/software-download-for-wave-desktop
GraphPad Prism 8.0	GraphPad Software	https://www.graphpad.com/scientific-software/prism/
Biorender	Biorender	https://app.biorender.com/

RESOURCE AVAILABILITY

Lead contact

Further information and requests for resources and reagents should be directed to and will be fulfilled by the lead contact, Zhi-Gang Zhang (zzhang@shsci.org).

Materials availability

All unique reagents generated in this study are available from the lead contact with a completed Materials Transfer Agreement.

Data and code availability

- The RNA-seq data generated in this study have been deposited in the Sequence Read Archive (SRA) repository under accession code PRJNA884743 [https://www.ncbi.nlm.nih.gov/bioproject/PRJNA884743]. The deposited RNA-seq data are publicly accessible as the date of publication.
- This paper does not report original code.
- Any additional information required to reanalyze the data reported in this paper is available from the lead contact upon request.

EXPERIMENTAL MODEL AND STUDY PARTICIPANT DETAILS

Cell lines

Mouse MC38 colorectal cancer cell line and Panc02 pancreatic cancer cell line were purchased from Cell bank of Chinese Academy of Sciences. EL4 cells were purchased from ATCC. MC38 and Panc02 cells were cultured in Dulbecco's modified Eagle's medium (DMEM) and EL4 cells were cultured in RPMI 1640, supplemented with 10% FBS and penicillin and streptomycin (100 U/ml each) at 37°C and 5% CO_2.

Mouse strains

Tph1$^{-/-}$, *Slc6a4*$^{fl/fl}$ and *Tgm2*$^{fl/fl}$ mice were purchased from Cyagen Biosciences. *Maoa*$^{fl/fl}$, *Cd8a*^{cre} and WT C57BL/6 mice were purchased from GemPharmatech Co., Ltd. Mice were bred and housed in Jiangsu University specific pathogen free (SPF) animal facility, and male mice were used between the ages of 8-10 weeks. All animal experiments were undertaken in accordance with protocols approved by Institutional Animal Care and Use Committee of Jiangsu University.

Please cite this article in press as: Wang et al., A GAPDH serotonylation system couples CD8+ T cell glycolytic metabolism to antitumor immunity, Molecular Cell (2023), https://doi.org/10.1016/j.molcel.2023.12.015

METHOD DETAILS

In vitro cell activation and flow cytometry analyses

$CD8^+$ T cells were isolated from the spleen of mice by $CD8^+$ magnetic bead selection (Miltenyi). αCD3 (2.5 μg/mL) + αCD28 (2.5 μg/mL) antibodies were used to activate the naïve $CD8^+$ T cells or EL4 cells in RPMI 1640, supplemented with 10% fetal bovine serum (FBS) at 37°C and 5% CO_2. Cells were treated with 5-HT (Sigma) at indicated concentrations in the presence or absence of HTR1B antagonist SB-224289 (Tocris), HTR1B agonist CP-94253 (Tocris), HTR7 antagonist SB-258719 (Tocris), HTR7 agonist AS-19 (Tocris), and TGMs inhibitor LDN-27219 (MCE). For proliferation studies, $CD8^+$ T cells were labelled with 1 μmol/L carboxyfluorescein succinimidyl ester (CFSE, Invitrogen) and then activated by αCD3/αCD28. The proliferation of $CD8^+$ T cells was detected with flow cytometry and analyzed by CFSE dilution. For intracellular staining, cells were treated with GolgiStop (BD) for 30 min and then fixed and permeabilized using the Fix/Perm kit (eBioscience) following the manufacturer's instructions. FITC anti-mouse IFN-γ (BD, 1:100), and anti-5-HT antibody (Sigma, 1:200) followed by secondary antibody (Abcam, 1:200) was performed for intracellular staining. Intracellular GAPDH Q262ser staining was performed with the similar procedure but without GolgiStop incubation.

Mouse tumor model

MC38 cells (0.5×10^6) or Panc02 cells (1×10^6) were suspended in 100 μL PBS and subcutaneously injected into the right flank of syngeneic mice (male, 8-10 weeks old). Tumor growth was monitored with an electronic calliper by measuring tumor size every 2 days. Tumor volumes were calculated as $1/2 \times \text{Length} \times \text{Width}^2$. Frequency and intracellular IFN-γ of $CD8^+$ T cells were detected at the 25 days (Panc02) and 18 days (MC38) after implantation.

In vivo cell isolation and flow cytometry

Mice were euthanized and fresh tissues were collected. Lymph nodes, spleens and thymuses were mechanically disrupted through disrupted through 70 μm Nylon mesh to release single cells. Bone marrow was flushed with PBS and triturated through 70 μm Nylon mesh. Tumor tissues were cut into small pieces with surgical scissors, digested with 2 mg/mL collagenase A (Sigma) and 1× DNase I (Sigma) for 20 min, quenched by FBS (Gibco) and filtered with 70 μm Nylon mesh.

For staining molecules expressed on cell surface, single cell suspensions from lymph nodes, spleens, thymuses, blood and bone marrow tissues were blocked with anti-mouse CD16/CD32 antibodies (Thermo Fisher) for 10 min and labeled with fluorophore-conjugated antibodies: PerCP/Cyanine5.5 anti-mouse CD45, PE anti-mouse CD8a, Alex Fluor 647 anti-mouse CD4, APC anti-mouse CD11b, Alex Fluor 488 anti-mouse F4/80 and PE-Cy7 anti-mouse Ly6G.

To enrich immunocytes in tumors, cells were centrifuged through a 37.5% Percoll (Sigma) at 600 × g for 35 min. For intracellular staining, single cell suspensions from tumor tissues were stimulated with Cell Stimulation Cocktail (Invitrogen) for 4 hours, and labeled with PerCP-Cyanine 5.5 anti-mouse CD 45, Brilliant Violet 605 anti-mouse CD8a. After fixation and permeabilization using the Fix/Perm kit (eBioscience) following the manufacturer's instructions, cells were labeled with FITC anti-mouse IFN-γ. To assess $CD8^+$ T cell infiltration in tumor tissues, single cell suspension of tumor tissues was stained with PerCP/Cyanine5.5 anti-mouse CD45 and BV605 anti-mouse CD8a. To analysis intracellular 5-HT content, MC38 or Pan02 cells were labeled by expressing eGFP. Cell suspension was stained with PerCP/Cyanine5.5 anti-mouse CD45 and Brilliant Violet anti-mouse CD8a, and then fixed with 2% paraformaldehyde (PFA), followed by 0.2% Triton X-100 for permeabilization. Cells were blocked with PBS containing 10% BSA for 1 hour, stained with anti-5-HT antibody (Sigma, 1:200) followed by Alexa Fluor 647-labeled secondary antibody (Abcam, 1:200) for 2 hours. Flow cytometry was performed in BD FACSCanto II.

Immunofluorescence staining and imaging

$CD8^+$ T cells or EL4 cells from each group were activated with αCD3/αCD28 for 24 hours. Panc02 cells and MC38 cells were treated with 5-HT for 24 hours. 2% PFA was used to fix cells, followed by 0.2% Triton X-100 for permeabilization. Cells were blocked with PBS containing 10% BSA for 1 hour, stained with anti-GAPDH (1:200), anti-GAPDH Q262ser (1:200), or TGM2 (1:200) overnight and secondary antibody (Abcam, 1:200) for 2 hours and mounted in DAPI-containing media (Vector Labs) for imaging on a laser scanning confocal microscope (Zeiss LSM800). The nuclear location of GAPDH of individual cells was analyzed with ImageJ software.

Immunohistochemical staining

Tumor tissues from each group were fixed with 4% PFA. Immunohistochemical staining was performed routinely. Tissues were dehydrated, embedded in paraffin and subsequently cut into 5 μm sections, and stained with anti-CD8a (Abcam), Ki67 (Abcam), and cleaved Caspase-3 (CST) after antigen retrieval. For quantification, six high magnification fields were blindly taken in each tissue section.

Stable transfection of EL4 cells

mCherry-fused lentiviruses expressing WT-GAPDH or Gln to Ala (Q46A, Q76A, Q183A, Q202A and Q262A) mutated GAPDH were constructed by GeneChem. EL4 cells were transfected at MOI 50. 6 μg/mL puromycin was add to the culture medium for 48 hours for selection. The overexpression efficiency was confirmed by Western blot analysis.

Metabolism assays

Extracellular acidification rate (ECAR) and oxygen consumption rate (OCR) were measured with the Seahorse XF96 Flux Analyser (Agilent) and Agilent Wave 2.6.1 software according to the manufacturer's instructions. $CD8^+$ T or EL4 cells from each group were stimulated with αCD3/αCD28 for 24 hours. 1 hour before testing, the media was replaced with assay media, and cells were seeded on plates. For ECAR test, 1 μmol/L oligomycin (O), 0.5 μmol/L carbonylcyanide p-trifluoromethoxyphenylhydrazone (FCCP), and 0.1 μmol/L antimycin A plus 0.5 μmol/L rotenone (A & R) were injected to the wells. For OCR test, 10 mmol/L glucose, 1 mol/L oligomycin (O), and 50 mmol/L 2-deoxyglucose (2-DG) were added to the wells. GAPDH (Abcam), ENO1 (Sigma) and LDHA (Sigma) glycolytic activities were analyzed with assay kits following the manufacturer's instructions. $CD8^+$ T or EL4 cells from each group were stimulated with αCD3/αCD28 for 24 or 72 hours. Cells were homogenized in cold Assay Buffer. Enzymatic activities were quantified according to the standard curve.

RNA sequencing

$CD8^+$ T cells were stimulated with αCD3/αCD28 for 24 hours, in the presence or absence of 100 μmol/L 5-HT and 25 μmol/L TGMs inhibitor LDN-27219. Total RNAs were isolated using the TRIzol reagent following the manufacturer's instructions and sent to OE Biotechnology for clustering and sequencing. RNA sequencing data were collected using NextSeq System Suite v2.2.0.

Real-time qPCR

$CD8^+$ T cells were activated with αCD3/αCD28 for indicated hours. Total RNA was extracted from naïve and activated $CD8^+$ T cells using Trizol reagent (Takara), followed by RNA reverse transcription with PrimeScript RT-PCR kit (Takara) according to the common protocols. Real-time PCR analyses were applied for gene expression study and SYBR Premix Ex Taq (Roche) was used to run PCR on a 7500 Real-time PCR system (Applied Biosystems) at the recommended thermal settings. Relative mRNA expression was calculated using the $2^{-\Delta\Delta Ct}$ method normalized to β-actin mRNA levels. Following primers were listed in Table S2.

5-PT immunoprecipitations and LC-MS/MS

Alkyne-functionalized 5-HT derivative 5-PT was prepared in house according to reported procedures.[34] $CD8^+$ T cells were stimulated with αCD3/αCD28 for 24 or 72 hours, in the presence or absence of 100 μmol/L 5-PT. Cells were homogenized in ice-cold lysis with RIPA buffer. Samples were quantified and 5% of the lysates were retained as inputs. To label serotonylated proteins, 5-PT was conjugated to a biotin–azide molecule (Thermo Fisher) using the copper-click chemistry following the manufacturer's instructions. Magnetic streptavidin beads were added into the CLICK reaction buffer. Following incubation, samples were placed on a magnet to collect the serotonylated proteins.

For LC-MS/MS analyses, SDT lysis buffer (4% SDS, 100 mmol/L DTT and 100 mmol/L TrisHCl) was added to the beads and boiled for 5 minutes. Centrifuge at 800g, the supernatants was mixed with UA buffer (8 mol/L Urea and 150 mmol/L Tris HCl) and transferred into ultrafiltration centrifuge tube for centrifugation 15 minutes at 12000 g. The UA buffer and 50mM NH4HCO3 were used to replace the buffer by centrifugation 15 min twice separately. Proteins were then digested with trypsin buffer for 16 hours at 37 °C. The digested peptides were desalted using C18 StageTip. Peptides were taken from each sample for chromatographic separation using an Easy nLC 1200 chromatographic system (Thermo) with a nanoliter flow rate. Buffer: A solution was 0.1% formic acid in water, and B solution was 0.1% formic acid, acetonitrile and water (wherein acetonitrile was 95%). The column is equilibrated with 100% liquid A. The sample is injected into Trap Column and then passed through the chromatographic analysis column for gradient separation, with a flow rate of 300 nL/min. The liquid phase separation gradient was as follows: 0 min-2 min, linear gradient of buffer B from 2 % to 8 %; 2 min-42 min, linear gradient of buffer B from 8 % to 28 %; 42 min-50 min, linear gradient of buffer B from 28 % to 40 %; 50 min-51 minutes, buffer B linear gradient from 40% to 100%; 51 min-60 min, buffer B maintained at 100%. Peptide separation was followed by Data Dependent Acquisition (DDA) mass spectrometry analysis using a Q-Exactive HF-X mass spectrometer (Thermo). The MS detection mode was positive and precursor ion MS scanning range was set as 300-1500 m/z. The full MS scan was resolution 60,000 at m/z 200, AGC target 3e6, and maximum IT 50 ms. The peptide MSMS were collected according to the 20 highest-intensity precursor ions after each full scan. The MS2 parameters were set as following: Resolution 15,000 at m/z 200, AGC target 1e5, Maximum IT 50 ms, MS2 activation type HCD, isolation window 1.6 m/z, Normalized collision energy 28. The mass spectrometry database search software used was MaxQuant 1.6.1.0. The protein database used was the Uniprot Protein Database, and the species was Mus musculus.

Enzymatic serotonylation assays

MDC (Sigma, 5 mmol/L 30432) or 5-HT (5 mmol/L) was transamidated to GAPDH (Novus, 10 μg NBP2-52622) or fibrinogen (Sigma, 10 μg F3879) protein by 0.25 μg functional TGM2 protein (Novus, 5418-TG-010), in a final volume of 25 μL enzymatic buffer (25 mM Tris-Cl, pH 8 and 5 mM CaCl2, plus protease inhibitors). The MDC serotonylation reaction was treated with TGM2 inhibitor cystamine (Sigma, 4 mmol/L) or competed with excess 5-HT (500 μmol/L). The reaction buffer was incubated at 37°C for 3 hours in the dark, heated to 98°C for 8 min in denaturing sample buffer before gel electrophoresis. Serotonylated proteins were visualized under UV light, followed by Coomassie staining for protein loading. Peptides of GAPDH were synthesized by Jiangsu JiTai Peptide Industry Science And Technology Co, Ltd. Transamidation of MDC or 5-HT to GAPDH peptides (10 μg) or full-length GAPDH (10 μg) was performed with the same procedures as above described GAPDH protein transamidation, followed by LC-MS/MS analyses of serotonylation.

Generation of GAPDH Q262ser antibody

With the help of PTM BIO, GAPDH Q262ser antibody was generated. GAPDH Q262ser peptide_1 (KKVVKQ$_{Ser}$ASEGP), GAPDH Q262ser peptide_2 (KKVVKQ$_{Ser}$ASEGPLK), and unmodified peptide (KKVVKQASEGPLK) were synthesized. LC-MS/MS analyses were performed to verify the peptides. Modified peptides were conjugated to keyhole limpet haemocyanin (KLH). Three New Zealand rabbits were immunized with each modified peptide for four times at Day 0, 21, 35 and 54. Serum from each rabbit was collected at Day 45, 50, 64 and 69 for verifying antibody titer by ELISA and Western blotting, and the optimal serum was selected for antibody purification. Peptide dot blots and western blots were performed to detect the specificity of GAPDH Q262ser antibody. For peptide dot blots experiments, Q262ser-modified and unmodified GAPDH 257-269 peptides were dotted in titration onto nitrocellulose membranes. After drying for 30 min, membrane was blocked with 5% BSA. Primary antibody (1:2000) and secondary antibody (1:10000) was incubated for 1 hour respectively, and imaged with an Enhanced Chemiluminiscence (ECL) kit (Abcam). For Western blot experiments, 5-HT (5 mmol/L) was transamidated to GAPDH (Novus, 10 μg) protein in the presence of 0.25 μg functional TGM2 protein (Novus), in a final volume of 25 μL enzymatic buffer (25 mM Tris-Cl, pH 8 and 5 mM $CaCl_2$, plus protease inhibitors). Protein samples were separated by 8-10% SDS-PAGE gel electrophoresis and transferred onto 0.22 μm NC membranes. After blocking with 5 % BSA diluted in Tris buffer saline plus 0.1% Tween 20 (TBST) for 1 hour at room temperature, membranes were incubated overnight with primary antibody (1:200), and 2 hours with secondary antibody (Immunoway, 1:10,000). Blots were visualized by the Bio-Rad system.

Immunoprecipitation and Western blotting

$CD8^+$ T cells or EL4 cells were activated with αCD3/αCD28 for 24 hours in the presence or absence of 5-HT (100 μmol/L). Cell lysates were prepared by using RIPA lysis buffer (Sigma) with addition of protease inhibitor cocktail (Sigma). TGMs inhibitor Cystamine (1 mmol/L, Sigma) was added for examining serotonylated proteins. Cell lysates were subjected to immunoprecipitation using anti-mCherry antibody (Abcam) with a Protein G Immunoprecipitation Kit (Thermo). Nuclear and cytoplastic protein was extracted using a Nuclear and Cytoplasmic Extraction Kit (Thermo). After total protein normalized, protein samples were separated by 8-10% SDS-PAGE gel electrophoresis and transferred onto 0.22 μm NC membranes. After blocking with 5 % BSA diluted in Tris buffer saline plus 0.1% Tween 20 (TBST) for 1 hour at room temperature, membranes were incubated overnight with primary antibody (1:200), and 2 hours with secondary antibody (Immunoway, 1:10,000). Blots were visualized by the Bio-Rad system.

Measurement of calcium flux

$CD8^+$ T cells were activated with αCD3/αCD28 for 1, 3, or 5 days. Washed with PBS, cells were loaded with Fluo-4/AM (10 μmol/L) at room temperature. After incubation for 30 min, cells were washed twice and then transferred to a 96-well plate and treated with HTR7 agonist AS-19 (50 μmol/L). Calcium signals were recorded using a fluorescent microplate. Increasement of fluorescence intensity (ΔF) was calculated.

ELISA

$CD8^+$ T cells were activated with αCD3/αCD28 for 24 hours. Intracellular 5-HT content was determined with an ELISA kit (Abcam) according to manufacturer's instructions. Total protein was determined by BCA assay, and used to normalize 5-HT content.

Production of CAR-T cells

Retroviral plasmids containing CAR constructs were generated as previously reported.[35] A fragment containing the anti-EGFRvIII single-chain variable fragment (scFv), CD28 transmembrane domain, and CD3 ζ intracellular domain was generated by overlap PCR and cloned into the pMSGV1 vector. For generating TPH1-overexpressing CAR plasmid, a cassette encoding TPH1 was inserted into this vector, as shown in Figure 7A. Retrovirus were produced by transient transfection of HEK-293T with a packaging plasmid. Supernatants containing retrovirus particles were collected at 48 and 72 hours after transfection and concentrated.

$CD3^+$ T cells were isolated from the spleen of mice by $CD3^+$ magnetic bead selection (Miltenyi). $CD3^+$ T cells were activated with αCD3/αCD28 Dynabeads (Life Technologies) for three days. The activated T cells were transfected with retroviral EGFRvIII/CAR, or TPH1-EGFRvIII/CAR. Plates were spined at 2000 ×g for 90 min at 32°C, and then transferred to an incubator and maintained overnight. 24 hours later, the medium replaced with fresh medium containing 20 IU/mL of murine IL-2. Transfection efficiency was evaluated by staining of $F(ab')_2$ fragment using an anti-Mouse IgG $F(ab')_2$ fragment specific antibody (Jackson) after 4-6 days of transduction. Cell number was counted at indicated time points. After transduction for 8 days, intracellular 5-HT was examined by ELISA, and GAPDH Q262ser was assessed by Western blotting as described above.

In vitro CAR-T cell cytotoxicity assay

EGFRvIII-luciferase-expressing MC38 cells were generated by lentiviral transduction, followed by puromycin selection for 5 days. After transduction for 8 days, CAR-T or TPH1-CAR-T cells were cocultured with target tumor cells at effector-to-target ratios of 1 : 1. After 24 hours incubation, luciferase activity was measured with a multi-mode microplate reader, and specific tumor killing activity was calculated. The supernatants were collected for examining IFN-γ by ELISA (Abcam).

In vivo CAR-T cell antitumor activity

0.5×10^6 EGFRvIII-expressing MC38 cells were suspended in 100 μL PBS and subcutaneously injected into the right flank of syngeneic mice (male, 8-10 weeks old). 5 days later, 1×10^7 EGFRvIII-specific CAR-T cells, or TPH1-overexpressing CAR-T cells were systemically injected to the tail vein. Tumor growth was monitored with an electronic calliper by measuring tumor size every 2 days. Tumor volumes were calculated as $1/2 \times \text{Length} \times \text{Width}^2$.

QUANTIFICATION AND STATISTICAL ANALYSIS

Data are presented as mean ± standard deviation. All statistics were carried out using GraphPad Prism 8. Student's t test was used to compare the differences between two groups. One-way analysis of variance (ANOVA) and Tukey's multiple comparisons test were used for the three or more groups comparisons. At least three independent biological replicates have been performed for each experiment. The number of independent experiments is indicated. $P < 0.05$ was considered to be statistically significant.